

Anatomy of the Feeding Apparatus of the Nurse Shark, *Ginglymostoma cirratum*

PHILIP J. MOTTA* AND CHERYL D. WILGA
Department of Biology, University of South Florida, Tampa, Florida

ABSTRACT The anatomy of the feeding apparatus of the nurse shark, *Ginglymostoma cirratum*, was investigated by gross dissection and computer axial tomography. The labial cartilages, jaws, jaw suspension, muscles, and ligaments of the head are described. Palatoquadrate cartilages articulate with the chondrocranium caudally by short, laterally projecting hyomandibulae and rostrally by ethmoorbital articulations. Short orbital processes of the palatoquadrates are joined to the ethmoid region of the chondrocranium by short, thin ethmopalatine ligaments. In addition, various ligaments, muscles, and the integument contribute to the suspension of the jaws. When the mouth is closed and the palatoquadrate retracted, the palatine process of the palatoquadrate is braced against the ventral surface of the nasal capsule and the ascending process of the palatoquadrate is in contact with the rostradorsal end of the suborbital shelf. When the mandible is depressed and the palatoquadrate protrudes slightly rostroventrally, the palatoquadrate moves away from the chondrocranium. A dual articulation of the quadratomandibular joint restricts lateral movement between the mandible and the palatoquadrate. The vertically oriented preorbitalis muscle spans the gape and is hypothesized to contribute to the generation of powerful crushing forces for its hard prey. The attachment of the preorbitalis to the prominent labial cartilages is also hypothesized to assist in the retraction of the labial cartilages during jaw closure. Separate levator palatoquadrati and spiracularis muscles, which are longitudinally oriented and attach the chondrocranium to the palatoquadrate, are hypothesized to assist in the retraction of the palatoquadrate during the recovery phase of feeding kinematics. Morphological specializations for suction feeding that contribute to large subambient suction pressures include hypertrophied coracohyoideus and coracobranchiales muscles to depress the hyoid and branchial arches, a small oral aperture with well-developed labial cartilages that occlude the gape laterally, and small teeth. *J. Morphol.* 241:33–60, 1999. © 1999 Wiley-Liss, Inc.

KEY WORDS: jaws; suction; muscles; ligaments; kinematics; jaw suspension

Functional studies on the feeding mechanisms of fishes and amphibians have given us insight into the evolution of vertebrate feeding mechanisms and behaviors (Lauder, '82; Lauder and Reilly, '88; Wainwright et al., '89; Reilly, '95). However, from a functional standpoint the Chondrichthyes are the least studied aquatic feeding vertebrates. Chondrichthyes are particularly interesting because they are derived from a common ancestor with the Teleostomi, before the Devonian, and have existed as a separate lineage for over 400 million years (Romer, '66; Schaeffer and Williams, '77;

Zangerl, '81; Carroll, '88). Sharks are particularly interesting because they include a variety of feeding morphologies and behaviors despite their relatively simple and conserved cranial morphology.

The skeletal elements associated with feeding in sharks are a fused neurocranium,

Contract grant sponsor: the National Science Foundation; Contract grant number: DEB 9117371.

*Correspondence to: Dr. Philip J. Motta, Department of Biology, University of South Florida, 4202 East Fowler Ave., Tampa, FL 33620. E-mail: motta@chuma.cas.usf.edu

a cleaver-shaped palatoquadrate, a mandible or Meckel's cartilage, a hyoid arch composed of three elements, and a branchial basket. The majority of Paleozoic sharks had a more terminal mouth, long jaws, amphistylic jaw suspension, and coronodont multicuspid teeth characterized by a distal-proximal series of subequal cusps fused into a multicuspid unit. These characters have induced speculation that these sharks grasped and tore their food. Prey capture in these ancestral sharks perhaps involved swimming over the prey (ram feeding), with less reliance on suction. In modern sharks, the jaws have shortened, resulting in greater bite force, the mouth has become more subterminal, and the suspensorium more maneuverable, permitting protrusion of the palatoquadrate (Schaeffer, '67; Moy-Thomas and Miles, '71; Compagno, '77; Zangerl, '81; Lund, '85; Carroll, '88; Lund and Grogan, '97).

Modern sharks have undergone a radiation in feeding types to include cutting, biting and gouging, filter feeding, biting and crushing, suction and grasping, and suction and crushing forms (Moss, '77; Motta et al., '97; Wilga and Motta, '98a). Specializations for capturing prey by suction have repeatedly arisen in numerous elasmobranch taxa, including the nurse shark *Ginglymostoma cirratum*, wobbegong *Orectolobus maculatus*, epaulette shark *Hemiscyllium ocellatum*, and whale shark *Rhincodon typus* (Orectolobiformes). The orectolobiform sharks, which are proposed to have a novel mechanism of jaw protrusion associated with suction feeding, appear to encompass more suction feeding species than other clades, and are apparently the most specialized suction feeders based on their anatomy and feeding kinematics (Tanaka, '73; Moss, '77; Wu, '94; Clark and Nelson, '97). The nurse shark, *G. cirratum*, is believed to demonstrate specialization for suction feeding including hypertrophied jaw abductor muscles, reduced dentition, well-developed labial cartilages that laterally occlude a small mouth, and generation of large subambient suction pressures (Bigelow and Schroeder, '48; Moss, '65, '77; Compagno, '73; Tanaka, '73; Dingerkus, '86; Wu, '94).

To understand the functional morphology of the feeding apparatus of any organism, knowledge of its anatomy is essential, including knowledge of the skeletal and connective tissue elements, the myology, and the kinematics during feeding. Compared to the Os-

teichthyes, there are fewer anatomical studies on elasmobranch feeding structures (see Motta and Wilga, '95, for a review), and even fewer studies that provide comprehensive descriptions of the musculature and connective tissue elements (Gadow, 1888; Daniel, '15; Allis, '23; Marinelli and Strenger, '59; Nobiling, '77; Motta and Wilga, '95), as well as functional studies on live, feeding elasmobranchs (Wu, '94; Motta et al., '97; Wilga and Motta, '98a,b; Ferry-Graham, '97, '98a,b). This study is part of a larger study on the functional morphology and evolution of shark feeding mechanisms. The goal of this study is to provide an anatomical analysis of the feeding apparatus of a suction feeding shark, the nurse shark, *Ginglymostoma cirratum*.

In the western Atlantic, *Ginglymostoma cirratum* is found from Cape Hatteras to Brazil, and in the east from West Africa to the Cape Verde Islands. In the eastern Pacific it is found from the Gulf of California to Peru (Castro, '83). The species primarily uses suction feeding to capture benthic invertebrates, including lobster, shrimp, crabs, squid, urchins, octopus, snails, and bivalves as well as small fishes (Bell and Nichols, '21; Gudger, '21; Bigelow and Schroeder, '48; Castro, '83; Compagno, '84). *G. cirratum* was chosen for this study because of its specialized suction feeding anatomy and behavior, its proposed novel jaw protrusion mechanism (Wu, '94), and the fact that it keeps well in captivity.

MATERIALS AND METHODS

Gross anatomy

A total of 21 *Ginglymostoma cirratum* specimens of both sexes, ranging in size from 40–252 cm total length (TL), were dissected. The specimens were acquired from the west and east coasts of Florida and the Florida Keys, primarily from commercial fishers and collectors. In some cases, sex could not be determined, as only the heads were available. Illustrations of fresh or preserved (formalin preserved, alcohol-glycerin stored) specimens were prepared by photographing dissected specimens and tracing the outlines of muscles and cartilages. Some illustrations were prepared with a camera lucida. Fiber direction of the muscles was verified independently by both authors.

Computer axial tomography

A series of images was taken of two male fresh specimens of *Ginglymostoma cirratum*

of 123 cm TL and 57 cm TL. The first series was taken of the smaller shark with the mouth in the closed, relaxed position, and the second series of the larger shark with the mouth propped open with the labial cartilages extended and the palatoquadrate maximally protruded to simulate positions of feeding movements revealed by video analysis. A Siemens DRH Computer Axial Tomography (CAT) scanner was used, with imaging performed in a transverse plane from the rostral margin of the head to the caudal end of the ceratohyal. Images were made every 4 mm with a 3 mm table, 3-sec exposure, and 280 milliamps at 125 kilovolts. An ISG Technologies Inc. CAMRA software program, version 5.0.1, reconstructed the images to produce a three-dimensional picture of the cartilaginous elements of the head.

Video and cine photography

Video and photographic images from a related feeding study of *Ginglymostoma cirratum* were used to visualize the position of the labial cartilages with the jaw in the maximally open position. A total of five male and female specimens, ranging from 64 to 98 cm TL, were fed pieces of Atlantic thread herring (*Opisthonema oglinum*) and crevalle jack (*Caranx hippos*) of approximately half the diameter of the mouth width. The sharks were filmed with a high-speed video camera (NAC HSV-200) at 200 fields/sec as well as with a Photosonics 1-PL 16 mm cine camera (with Kodak Tri-X reversal film) at 200 frames/sec. Illumination was provided by approximately 3,000 watts of quartz-halogen light. Video images were analyzed with a Panasonic AG-1970 video player and monitor and cine images with an LW Athena analysis projector.

Anatomical nomenclature

The anatomical nomenclature for the chondrocranium and visceral arches primarily follows that of Compagno ('88), with reference to Gegenbaur (1872), Daniel ('34), and Allis ('13, '14, '23). However, there is no standardized nomenclature for chondrocranial structures in Chondrichthyes (Compagno, '88).

Nomenclature for the connective tissue elements of elasmobranchs primarily follows Gadow (1888), with reference to Goodey ('10), Daniel ('15), Allis ('23), Moss ('72), and Nobiling ('77) (Table 1). However, descriptions of the ligaments and their synonyms are often

ambiguous. We only describe and name distinct band-like ligaments and tendons. Diffuse connective tissue elements or those with extremely short fibers (such as in joint capsules) are not described. The muscle terminology is primarily taken from Luther ('09), with modifications by Allis ('23), Daniel ('34), Edgeworth ('35), and Lightoller ('39) (Table 2). Embryological muscle groupings follow those of Miyake et al. ('92). Proximal and distal refer to the distance of point of attachment of the cartilage to the chondrocranium.

RESULTS

The orectolobid chondrocranium and jaws, as pertaining to feeding, are described briefly by Compagno ('77, '88), Moss ('77), Dingerkus ('86), and Wu ('94). Therefore, only the cartilaginous elements of the jaws, jaw suspension, joints, and connective tissue elements of the jaw apparatus, which are functionally important but lacking in detail in the literature, are described in detail here.

Jaws and labial cartilages

The paired palatoquadrate and mandibular cartilages are each joined by symphyses rostrally. The palatoquadrate bears a rostral palatine process and a caudal quadrate process. A small orbital process projects from the medial surface of the ascending process of the palatoquadrate, rostral to the attachment of the inner quadratomandibular ligament (LQI) (Figs. 1-4).

The mandible has a semicircular ridge that projects laterally from its caudal end, the sustentaculum (SUST) of Gegenbaur (1872) (see also Denison, '37) (Figs. 1, 4). The dorsal surface of the sustentaculum forms the socket of the lateral quadratomandibular joint (see below). Medial to the sustentaculum is the large mandibular knob (MK) (see Daniel, '15; Motta and Wilga, '95), the caudal surface of which bears the socket for the hyomandibulomandibular joint (Figs. 2, 3). Rostral to the mandibular knob, on the dorsal surface of the palatoquadrate, is the medial quadratomandibular joint.

The quadratomandibular diarthrodial joint has a double articulation. The lateral quadratomandibular joint between the sustentaculum of the mandible and the palatoquadrate lies in a frontal plane. This joint is ellipsoidal, such that it resists lateral movement between the mandible and the palatoquadrate. The medial quadratomandibular joint lies rostromedial to the latter joint and lies in the sagittal plane, further restricting

TABLE 1. (Continued)

Hyoidioman- dibular		mandibu- lohyal	hyoideoman- dibulare laterale inferius		hyoideoman- dibulare laterale inferius complexum	mandibulo- ceratohyal	mandibulo- hyoideum	hyoideoman- dibulare	
Medial hyoid- ioman- dibular	ausseres hyoman- dibular	meta- pterygoid	hyoideoman- dibulare mediale + hyoman- dibulohyoi- deum pos- terius	inferior postspi- racular				complexum	
Internal hyoidio- mandibular			mandibulo- hyoideum internum				glenoidale	mediale ?	
External hyoid-man- dibular*			hyoideoman- dibulare laterale superius		mandibulo- hyoideum externum		mandibulo- hyoman- dibulare externum		
Hyomandibu- locerato- hyoman- dibular			hyomandibu- loman dibu- lare						
Hyomandibu- locerato- hyal					quadratohy- oideo internum	hyomandibu- lohyoideum	quadrato- hyoideo internum	hyomandibu- lohyoideum	hyomandibu- lohyoideum
Palato- quadra- tolabial									
Ceratohyoba- sihyal									
Knob-labium									

X denotes the same nomenclature used in this work and that of Motta and Wilga ('95).

*These ligaments are present in the lemon shark but not in the nurse shark.

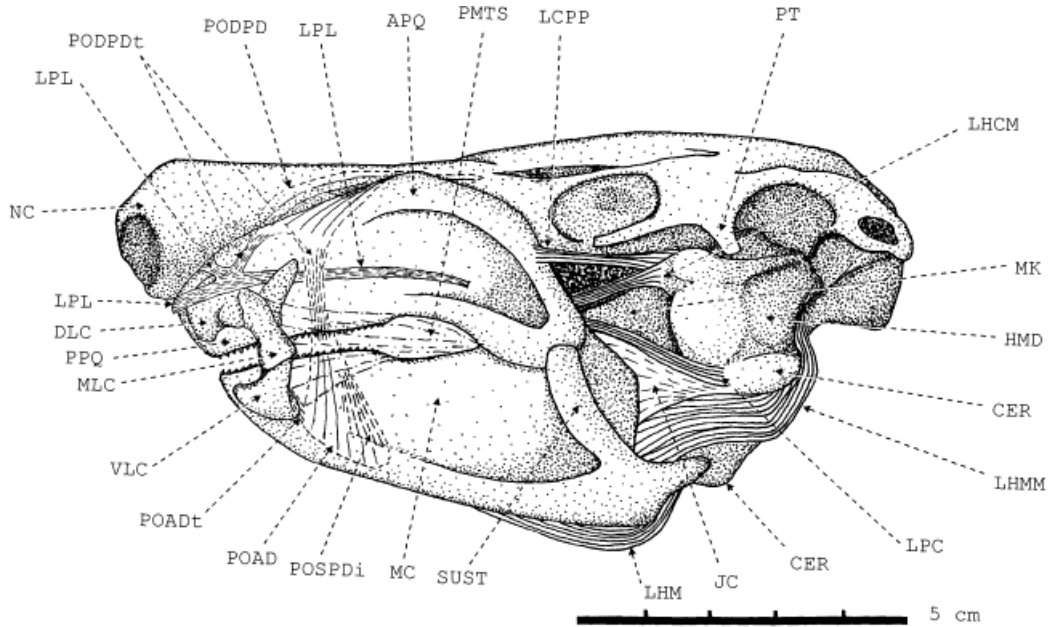


Fig. 1. Left lateral view of the chondrocranium, jaws, labial cartilages, and hyoid arch of a 114-cm TL male *Ginglymostoma cirratum* with the skin and muscles removed. Tendons and ligaments are indicated as well as the outline of the anterior division of the preorbitalis and the deep head of the posterior division of the preorbitalis. APQ, ascending process of palatoquadrate; CER, ceratohyal; DLC, dorsal labial cartilage; HMD, hyomandibula; JC, joint capsule; LCPP, chondrocraniopalatoquadrate ligament; LHCM, hyomandibuloceratohyomandibular ligament; LHM, hyoidmandibular ligament; LHMM, medial hyoidmandibular ligament; LPC, pala-

toquadratohyal ligament; LPL, palatoquadratal labial ligament; MC, mandibular cartilage; MK, mandibular knob; MLC, medial labial cartilage; NC, nasal capsule; PMTS, palatoquadratomandibular connective tissue sheath; POAD, anterior division of preorbitalis; POADt, tendon of anterior division of preorbitalis; PODPD, deep head of posterior division of preorbitalis; PODPDt, tendon of deep head of posterior division of preorbitalis; POSPDi, insertion of superficial head of posterior division of preorbitalis; PPQ, palatine process of palatoquadrate; PT, postorbital process; SUST, sustenaculum; VLC, ventral labial cartilage.

lateral displacement of the jaws. The medial quadratomandibular joint is similar to a gliding joint in having a shallow fossa in the palatoquadrate and a small, circular condyle on the mandible (Fig. 4).

The labial cartilages, which are placed rostrally on the jaws (Compagno, '88), are composed of three cartilages, a dorsal, medial, and ventral one. The proximal ends of the dorsal and ventral labial cartilages are ligamentously connected to the palatoquadrate and mandible, respectively, with their distal ends connected ligamentously to the medial labial cartilage. The medial labial cartilage has a medially directed process that abuts the palatoquadrate and acts as a brace between the labial cartilages and the jaw (Fig. 1).

Jaw suspension and related joints

The jaws are connected to the chondrocranium caudally by the hyomandibulae and

rostrally at the ethmopalatine joint (Figs. 1, 2). Various ligaments, muscles, and the integument contribute to the suspension of the jaws. The ethmopalatine joint articulates the palatoquadrate to the ethmoid region of the chondrocranium. The short orbital process articulates with a groove formed by the lateral edge of the antorbital shelf of the chondrocranium (Fig. 3). The articular facets are enclosed within a joint capsule formed in part by the thin sleeve-like ethmopalatine ligament. In addition, the palatine process of the palatoquadrate rests against the ventral surface of the nasal capsule, and the ascending process of the palatoquadrate rests against the rostradorsal end of the suborbital shelf. During jaw opening, the ethmopalatine joint permits gliding of the palatoquadrate on the chondrocranium such that the palatoquadrate protrudes slightly from the head in a rostroventral direction.

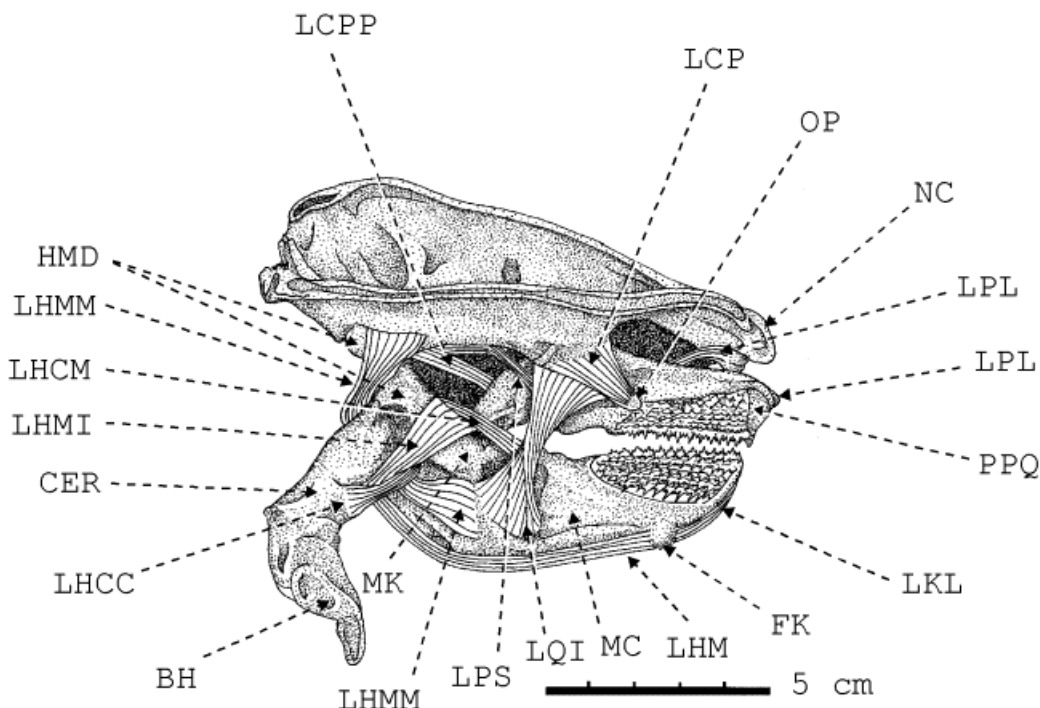


Fig. 2. Medial view of the chondrocranium, palatoquadrate, and mandible with attached hyomandibula, ceratohyal and basihyal from a 114-cm TL male *Ginglymostoma cirratum*. Basihyal is cut mid-sagittally and labial cartilages are removed. Hyoid arch elements are overextended to expose the ligaments and the CPTS, MHTS, and PMTS ligaments are removed. BH, basihyal; CER, ceratohyal; FK, fibrous knob; HMD, hyomandibula; LCP, ethmopalatine ligament; LCPP, chondrocraniopalatoquadrate ligament; LHCC, hyoman-

dibuloceratohyal ligament; LHCM, hyomandibuloceratohyal ligament; LHM, hyoidiomandibular ligament; LHMI, internal hyoidiomandibular ligament; LHMM, medial hyoidiomandibular ligament; LKL, knoblabium ligament; LPL, palatoquadratolabial ligament; LPS, palatoquadrate sheath ligament; LQI, inner quadratomandibular ligament; MC, mandibular cartilage; MK, mandibular knob; NC, nasal capsule; OP, orbital process of palatoquadrate; PPQ, palatine process of palatoquadrate.

The short and stout hyomandibulae project laterally from the chondrocranium. At the joint between the hyomandibula and the chondrocranium, the hyomandibula has a rostral and a caudal condyle (Fig. 3). The corresponding chondrocranial fossae are ellipsoidal, with their longitudinal axes oriented rostroventrally. This diarthrosis allows the distal end of the hyomandibula to move rostroventrally, but restricts twisting about its longitudinal axis. The distal end of the hyomandibula articulates with the mandible rostrolaterally and with the ceratohyal ventrally (Figs. 1–3). The hyomandibulomandibular joint is a diarthrosis composed of a shallow socket on the mandibular knob and a condyle on the hyomandibula. The hyomandibuloceratohyal articulation is a syndesmosis (Fig. 1). The union between the hyomandibula, mandible, and ceratohyal is tightly surrounded by numerous ligaments (see Con-

nective tissue elements, below). The medially located basihyal is joined to the ceratohyal by a syndesmosis, and lies in the angle of the mandible (Figs. 2, 3, 5).

Kinematics of jaws and hyoid arch

CAT scans and dissection reveal that when the mouth is closed and the palatoquadrate retracted, the palatine process of the palatoquadrate rests against the ventral surface of the nasal capsule, and the ascending process of the palatoquadrate rests against the rostrodorsal end of the suborbital shelf (Fig. 6). During manual depression of the mandible and protrusion of the palatoquadrate, the palatine process of the palatoquadrate moves ventrally and slightly rostrally. The palatoquadrate loses its rostral connection to the neurocranium and the folded ethmopalatine ligament is extended. Concomitantly, the distal end of the hyomandibula pivots ven-

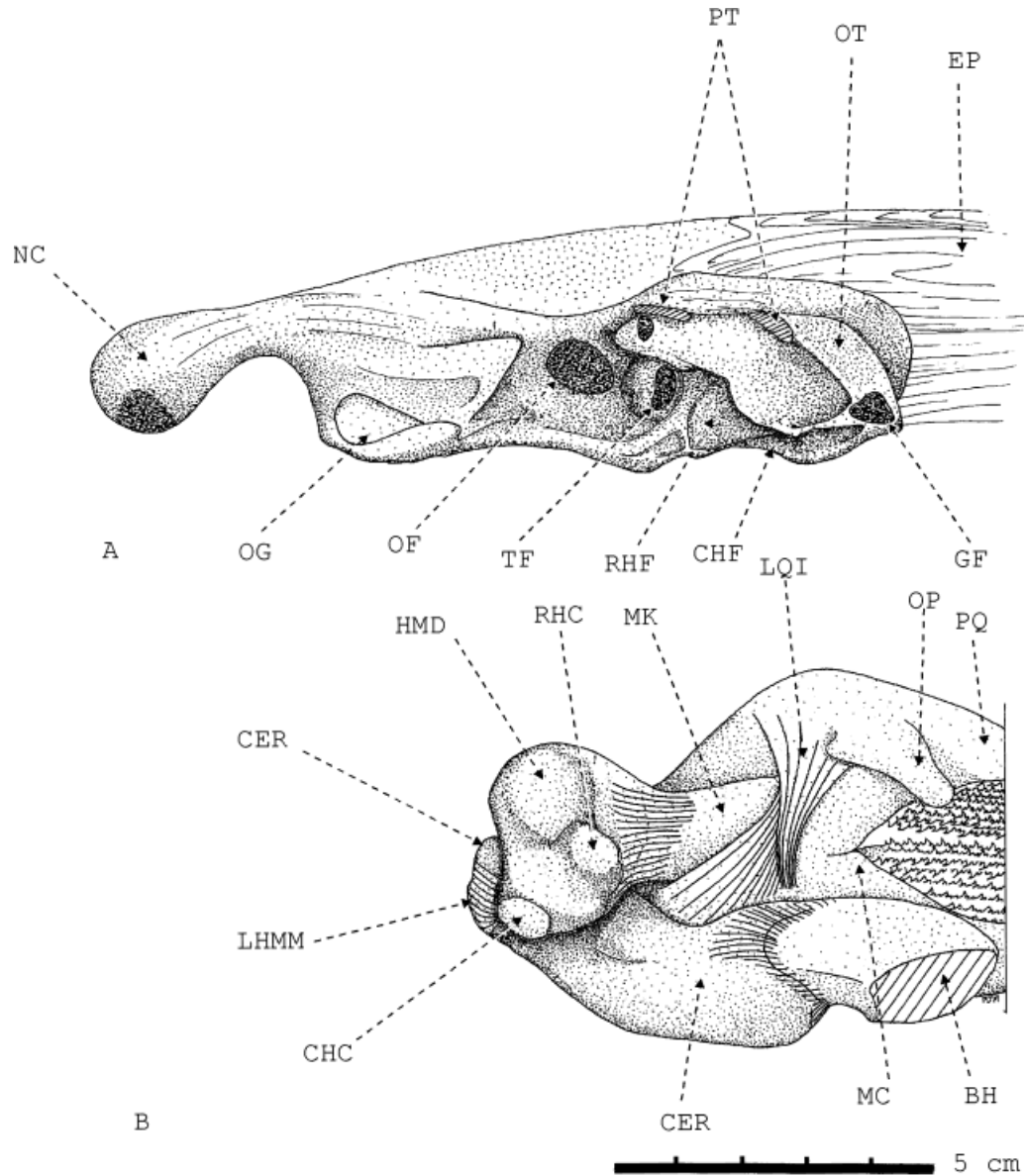


Fig. 3. **A:** Left lateral view of the chondrocranium. **B:** Medial view of the left hyoid arch and jaws, illustrating the articulating surfaces between the hyomandibula and the chondrocranium, and the joint between the ceratohyal and basihyal in a 69-cm TL male *Ginglymostoma cirratum*. The skin, muscles, and distal portion of the postorbital process have been removed, the basihyal cut mid-sagittally, and the majority of ligaments removed to expose the cartilages. BH, basihyal; CER, ceratohyal; CHC, caudal hyomandibular condyle; CHF,

caudal hyomandibular fossa; EP, epaxialis; GF, glosso-pharyngeal foramen; HMD, hyomandibula; LHMM, medial hyoideomandibular ligament; LQI, inner quadrato-mandibular ligament; MC, mandibular cartilage; MK, mandibular knob; NC, nasal capsule; OF, optic foramen; OG, orbital groove; OP, orbital process of palatoquadrate; OT, otic capsule; PQ, palatoquadrate; PT, postorbital process; RHC, rostral hyomandibular condyle; RHF, rostral hyomandibular fossa; TF, trigeminofacial foramen.

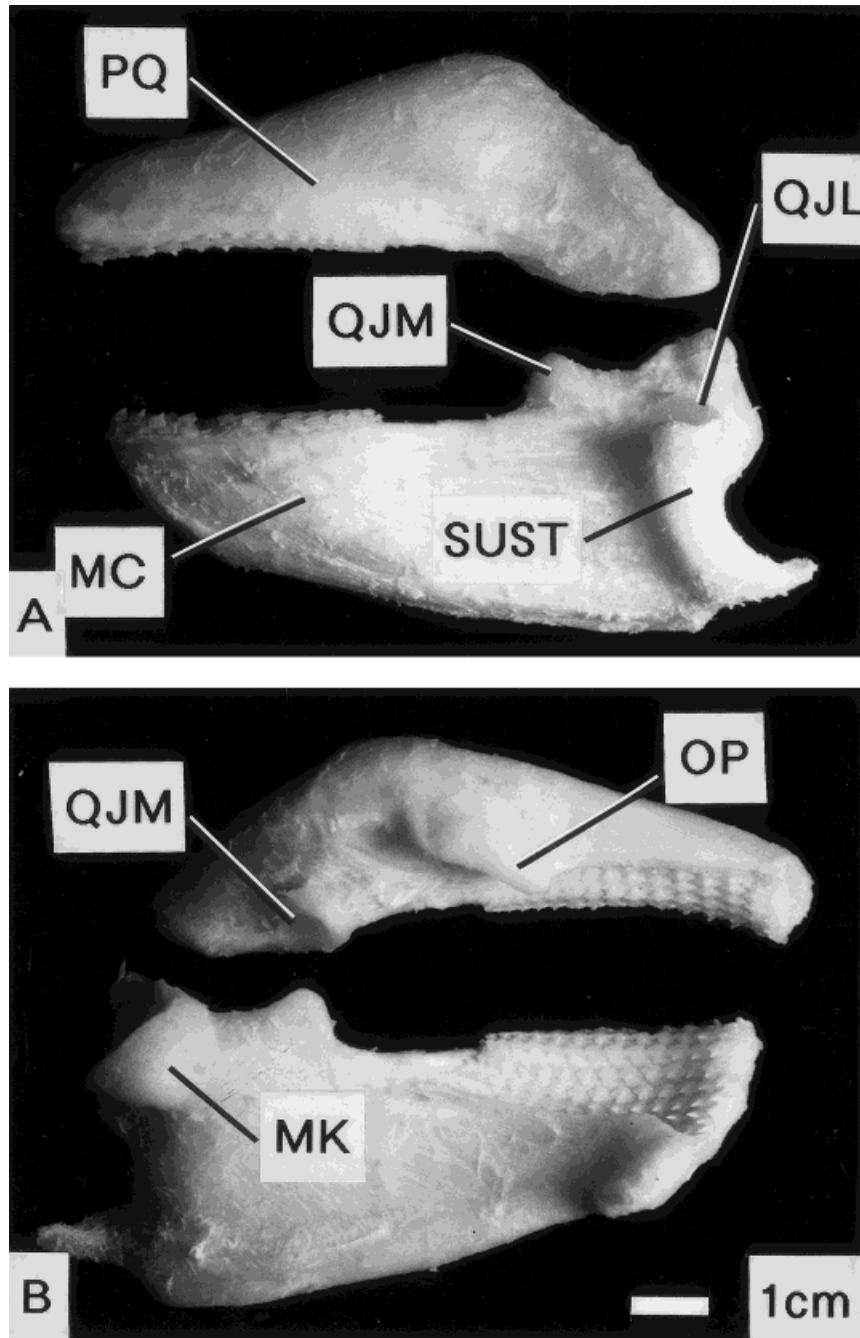


Fig. 4. A: Left lateral view of the palatoquadrate and mandible of an 123-cm TL male *Ginglymostoma cirratum* (ligaments and muscles removed) with the upper and lower jaw separated to expose the lateral and medial quadratomandibular joints. B: Medial view of the

same. MC, mandibular cartilage; MK, mandibular knob; OP, orbital process of palatoquadrate; PQ, palatoquadrate; QJL, lateral quadratomandibular joint; QJM, medial quadratomandibular joint; SUST, sustentaculum.

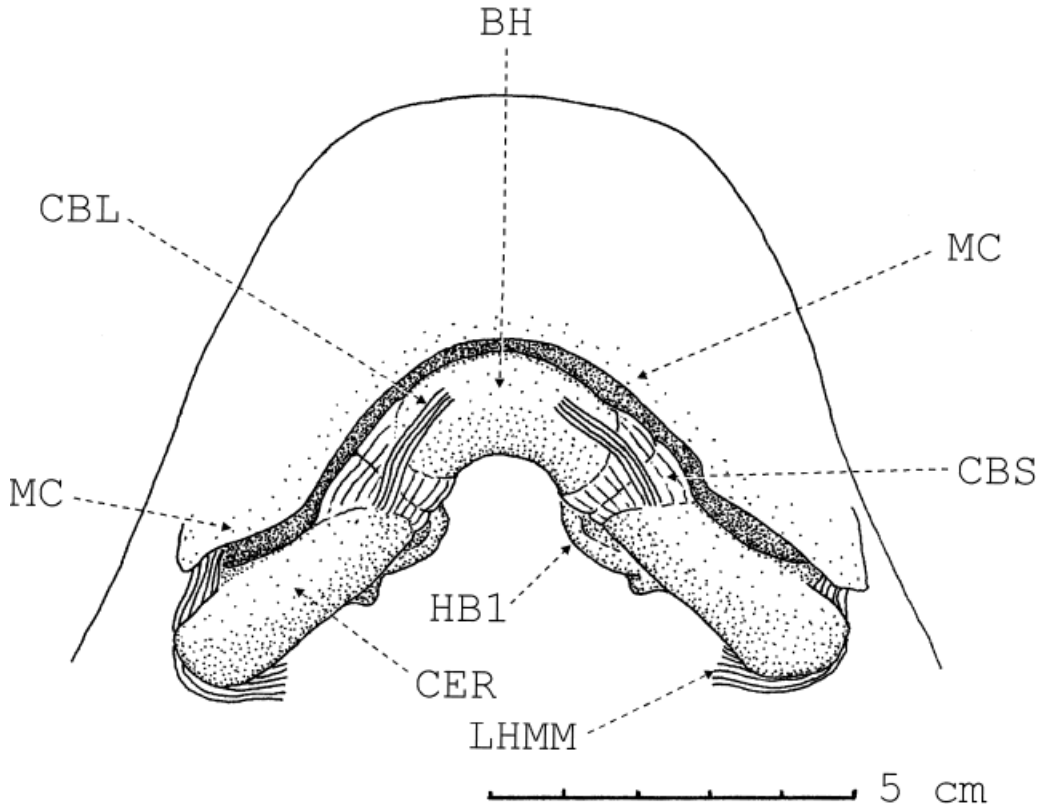


Fig. 5. Ventral view of the hyoid arch of a 64-cm TL female *Ginglymostoma cirratum* illustrating the ceratohyobasihyal articulation. The skin, muscles, and the mandibulothyoid connective tissue sheath have been removed and the hyoid arch depressed ventral to the mandible to expose the cartilages and joints. The outline

of the head and ventral margin of the mandible is indicated. BH, basihyal; CBL, ceratohyobasihyal ligament; CBS, ceratohyobasihyal syndesmosis; CER, ceratohyal; HB1, first hypobranchial; LHMM, medial hyoid-omandibular ligament; MC, mandibular cartilage.

trally and slightly rostrally. The hyomandibuloceratohyal joint is tightly bound to the mandible in the region of the quadratomandibular joint. Therefore, as the hyomandibula pivots the palatoquadrate is moved ventrally and slightly rostrally through its connection with the mandible, resulting in protrusion of the palatoquadrate rostroventrally.

The distal end of the ceratohyal rotates caudoventrally such that the ceratohyal is almost perpendicular to the chondrocranium. The basihyal moves from its juxtaposition just caudal to the mandibular symphysis to a more caudoventral position. When the mouth is maximally open, the basihyal and ceratohyal protrude ventrally, caudal to the mandible.

Video analysis of live feeding sharks and manual manipulation of fresh specimens reveals that in the closed position the labial

cartilages form a U, with the concave side oriented rostrally. This is not well defined on the CAT scans due to limited resolution of the labial cartilages. As the jaw opens, the medial labial cartilage and the distal ends of the dorsal and ventral labial cartilages swing rostrally to lie almost in the transverse plane. Together with the palatoquadratomandibular connective tissue sheath (PMTS), they laterally occlude the gape (Fig. 7). The labial cartilages and the rostral ends of the jaws form a laterally enclosed and somewhat round oral aperture when the mouth is open.

Connective tissue elements

Ligaments of the chondrocraniopalatoquadrate articulation

Ethmopalatine ligament (LCP; Fig. 2).

This short ligament arises from the lateral edges of the antorbital ledge and extends laterally to the orbital process of the

palatoquadrate. A stout, elastic portion of the ligament attaches to the caudal aspect of the orbital process, and a thin, fibrous outer sleeve (LCP in Fig. 2) completely envelops it.

Chondrocraniopalatoquadrate ligament (LCPP; Figs. 1, 2, 8). This arises from the caudal margin of the chondrocraniopalatoquadrate connective tissue sheath (CPTS) and caudal margins of the suborbital shelf. It extends rostrally to the dorsomedial surface of the palatoquadrate caudal to the ascending process and dorsal to the palatoquadratomandibular articulations.

Palatoquadrate sheath ligament (LPS; Figs. 2, 8). This arises from the medial margin of CPTS caudal to the antorbital ledge. It extends rostrally to the medial surface of the ascending process of the palatoquadrate.

Chondrocraniopalatoquadrate connective tissue sheath (CPTS; Fig. 8). This broad connective tissue sheath arises from the ventral surface of the hyomandibula and the ventrolateral and rostroventral surfaces of the chondrocranium; specifically, from the suborbital shelf, antorbital ledge, nasal capsule, and subnasal plate. It attaches to the medial surface of the palatoquadrate throughout its length.

Palatoquadratomandibular connective tissue sheath (PMTS; Figs. 1, 7). The sheath is continuous with the CPTS. The PMTS spans the angle of the mouth, encompasses the labial cartilages, and forms the internal surface of the labial folds. This thick connective tissue sheath overlies the labial margins of the palatoquadrate and mandible.

Mandibulohyoid connective tissue sheath (MHTS; not illustrated). MHTS (ventral component of CPTS of Motta and Wilga, '95) is continuous with CPTS and PMTS. It arises from the dorsolateral surface of the ceratohyal and the rostral and lateral edge of the basihyal. It extends to the ventromedial surface of the mandible and overlies the developing teeth. There are two oral valves arising from it on each side of the oral chamber. The large, caudal valve lies between the basihyal, ceratohyal, and the mandible. The small, more rostral valve is continuous with the connective tissue overlying the developing teeth. The mandibulohyoid connective tissue sheath binds the "tongue" to the floor of the mouth.

Ligaments of the palatoquadratomandibular articulation

Inner quadratomandibular ligament (LQI; Figs. 2, 3). Dorsally, this large ligament has a broad attachment on the medial surface of the palatoquadrate, caudal to the orbital process. It extends ventrally to the ventromedial surface of the mandible with some fibers attaching to the rostral surface of the mandibular knob. The ligament twists 180° as it extends ventrally such that the rostral fibers on the palatoquadrate attach caudally on the mandible and vice versa.

Ligaments of the palatoquadratoceratohyal articulation

Palatoquadratoceratohyal ligament (LPC; Figs. 1, 8). This thin ligament arises from the dorsolateral proximal end of the ceratohyal and extends rostromedially to attach to the medial surface of the palatoquadrate dorsal to the medial quadratomandibular joint.

Ligaments of the ceratohyomandibular articulation

Hyoidiomandibular ligament (LHM; Figs. 1, 2, 9). This arises from the rostrolateral edge of the proximal ceratohyal. It attaches to the ventral edge of the mandible, superficial to MHTS, and continues rostrally to eventually attach to a fibrous knob. This fibrous knob lies adjacent to the caudoverventral surface of the mandibular symphysis and is connected to the symphysis and both mandibles by dense connective tissue. The knob-labium ligament (LKL; Figs. 2, 9) arises from the fibrous knob and fans out, attaching to the dense connective tissue of the ventral labium.

Medial hyoidiomandibular ligament (LHMM; Figs. 1, 2, 3, 5, 8, 9). This thick ligament is the largest ligament of the cranium. It has two attachments at its proximal end. The longer head arises from the ventral surface of the chondrocranium from the region of the hyomandibulochondrocranial joint to the caudal suborbital shelf. The shorter head arises from the ventral surface of the hyomandibula. The long head extends ventrally to merge with the short head, then extends laterally to wrap around the proximal end of the ceratohyal to which some of the deeper fibers are attached. Coursing rostroventrally, it attaches to the caudal surface of the sustentaculum and the caudomedial surface of the mandible.

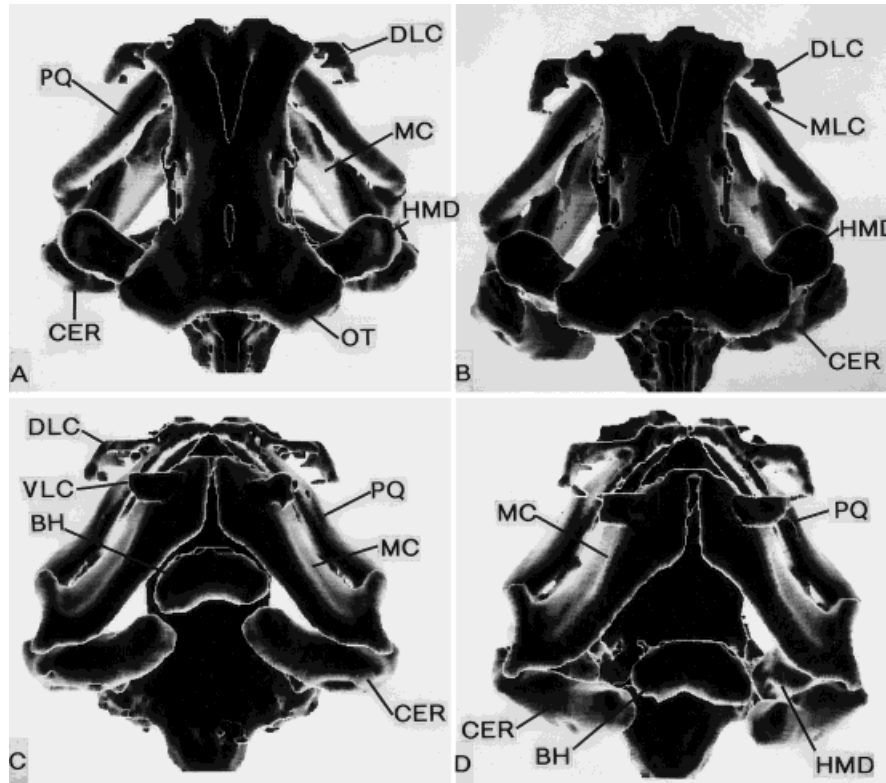


Fig. 6. The chondrocranium, mandibular, and hyoid arches of two intact *Ginglymostoma cirratum* heads reconstructed through CAT scan. Left figures with jaw closed are from a male 57-cm TL shark and right figures with mandible manually depressed, labial cartilages extended, and palatoquadrate maximally protruded are from a male 123-cm TL shark. **A:** Dorsal view indicating position of the hyomandibula and ceratohyal. **B:** Dorsal view indicating position of the hyomandibula and ceratohyal. **C:** Ventral view showing position of the ceratohyal and rostral position of the basihyal. **D:** Ventral view indicating the relative position of the basihyal and ceratohyal when the mouth is open. **E:** Left lateral view illustrating jaw closed with the hyomandibula, ceratohyal and labial cartilages in the resting position. **F:** Left lateral view with the palatoquadrate slightly protruded, the distal end of the hyomandibula pivoted ventrally

and slightly rostrally, the distal ceratohyal pivoted caudoventrally, and the basihyal and distal ceratohyal bulging ventrally below the head. The labial cartilages swing rostrally to lie almost in a vertical orientation although this is not well defined in these images. **G:** Right mid-sagittal view showing the position of the ceratohyal and basihyal and the palatoquadrate in the resting position. **H:** Right mid-sagittal view with the mouth open and palatoquadrate protruded, showing the caudoventral excursion of the ceratohyal and basihyal. APQ, ascending process of palatoquadrate; BH, basihyal; CER, ceratohyal; DLC, dorsal labial cartilage; HMD, hyomandibula; MC, mandibular cartilage; MLC, medial labial cartilage; NC, nasal capsule; OT, otic capsule; PPQ, palatine process of palatoquadrate; PQ, palatoquadrate; SUST, sustentaculum; VLC, ventral labial cartilage.

Internal hyoidiomandibular ligament (LHMI; Fig. 2). Arising on the proximal ceratohyal caudal to the attachment of the hyomandibuloceratohyal ligament (LHCC), this ligament extends dorsally to attach to the medial aspect of the mandibular knob.

Ligaments of the hyomandibulomandibular articulation

Hyomandibuloceratohyal ligament (LHCC; Figs. 1, 2, 8). This thin ligament arises from the rostradorsal sur-

face of the distal hyomandibula. The ligament then extends ventromedially, attaching to the dorsomedial surface of the mandibular knob medial to the inner quadratomandibular ligament (LQI) ligament.

Ligaments of the hyomandibuloceratohyal articulation

Hyomandibuloceratohyal ligament (LHCC; Fig. 2). This thick ligament arises from the lateral end of the hyomandibula and lateral hyomandibuloceratohyal joint cap-

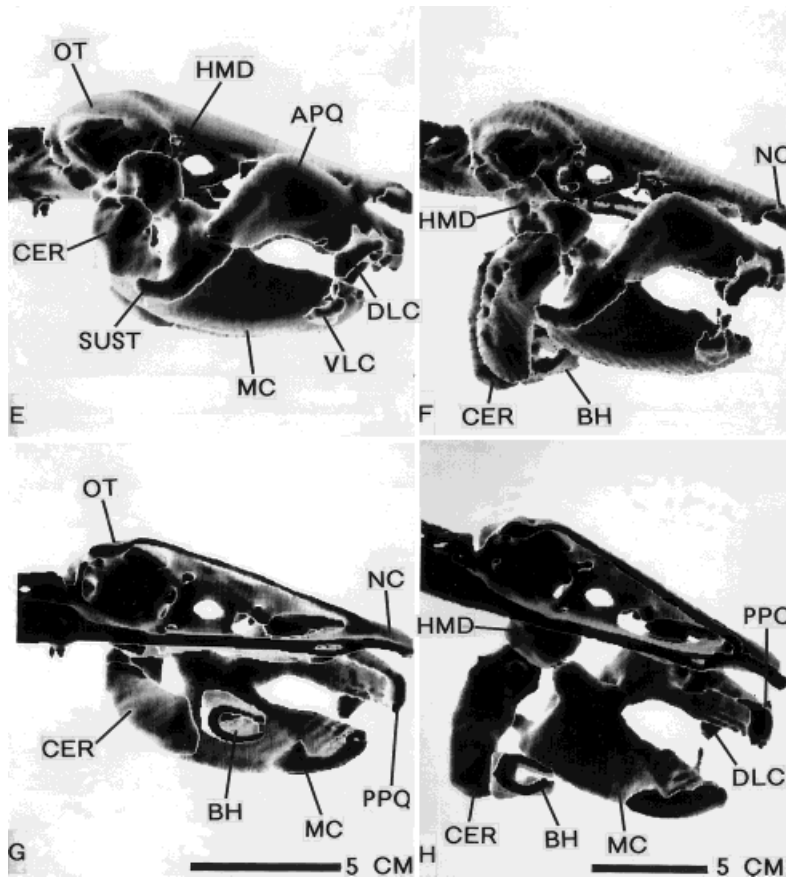


Figure 6 (Continued)

sule. Wrapping around the joint capsule, it extends rostroventrally to attach to the dorsolateral surface of the ceratohyal nearly at its mid-length. Viewed medially, this ligament lies in the angle of the ceratohyal.

Ligaments of the palatoquadrato-labial articulation

Palatoquadrato-labial ligament (LPL; Figs. 1, 2). Arising on the mid-lateral surface of the palatoquadrate, this ligament extends rostradorsally along the surface of the palatoquadrate under the medially directed process of the medial labial cartilage. Rostral to this, some fibers of the cranial tendon of the deep head of the posterior division of the preorbitalis merge with it. The LPL then continues rostrally and some of the fibers attach to the ventromedial surface of the nasal capsule, while the remaining fibers cross over the dorsal labial cartilage, span

the rostral surface of the palatoquadrate, and merge with the fibers of its contralateral counterpart.

Ligaments of the ceratohyobasihyal articulation

Ceratohyobasihyal ligament (CBL; Fig. 5).

This thin, short ligament arises from the rostrolateral edge of the distal ceratohyal. Lying deep to CPTS, it extends rostrally to attach to the rostrolateral edge of the ventral surface of the basihyal.

Head musculature

Muscles of the mandibular muscle plate

Levator palatoquadratii (LP; Fig. 10).

This muscle lies deep to the orbit and is a compound muscle composed of the *levator palatoquadratii* proper and the first dorsal constrictor, the *spiracularis* (Table 2). Both muscles lie almost in the frontal plane. The

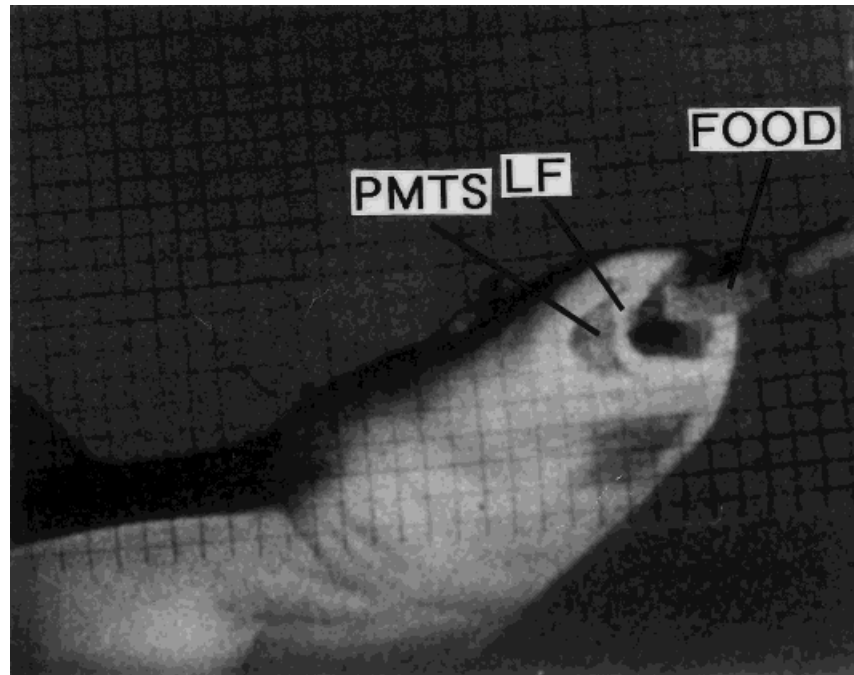


Fig. 7. Craniolateral view of a 98-cm TL male *Ginglymostoma cirratum* suction feeding on a piece of fish. Labial folds and palatoquadramandibular connective tissue sheath are laterally occluding the rostrally directed gape. Grid in front of shark indicates 1-cm squares. LF, labial fold; PMTS, palatoquadramandibular connective tissue sheath.

spiracularis has a muscular and tendinous origin from the otic capsule caudoventral to the postorbital process. Its fibers run rostrally to insert by a large tendon on the ascending process of the palatoquadrate. The levator palatoquadratii originates on the otic capsule ventral to the base of the postorbital process, immediately rostromedial to the origin of the spiracularis. Its fibers course rostrolaterally to insert by a muscular insertion deep to the inner quadramandibular ligament (LQI) on the ventromedial edge of the ascending process of the palatoquadrate.

Adductor mandibulae complex. This is considered by Lightoller ('39) to be a functional complex comprised of the preorbitalis and quadramandibularis muscles.

Preorbitalis. This muscle is divided into "anterior" and "posterior" divisions (Moss, '65), with the posterior division again being distinctly divided into two heads. The anterior division of the preorbitalis (POAD; Figs. 1, 11) originates on the ventral rim of the mandible, partially overlying the insertion of the rostral quadramandibularis divi-

sion (QM1). The rostral portion has a tendinous connection to the caudal surface of the ventral labial cartilage and the labial fold (Fig. 1). The majority of this division courses dorsally to merge with the insertional tendon of the deep head of the posterior division of the preorbitalis. This common tendon lies caudal to the palatoquadramandibular connective tissue sheath that spans the angle of the mouth and forms the labial folds.

The superficial head of the posterior division of the preorbitalis (POSPD; Figs. 12, 13) originates on the dorsal surface of the neurocranium from the anterior fontanelle to the parietal fossa, on the rostral edge of the epaxialis, and on the dorsal surface of the proximal postorbital process. Some fibers from the deep head merge with fibers of the superficial head as it descends over the margin of the palatoquadrate. The superficial head inserts by a large thick tendon on the craniolateral edge of the ventral rim of the mandible (POSPDi; Fig. 1).

The deep head of the posterior division of the preorbitalis (PODPD; Fig. 1) is deep to

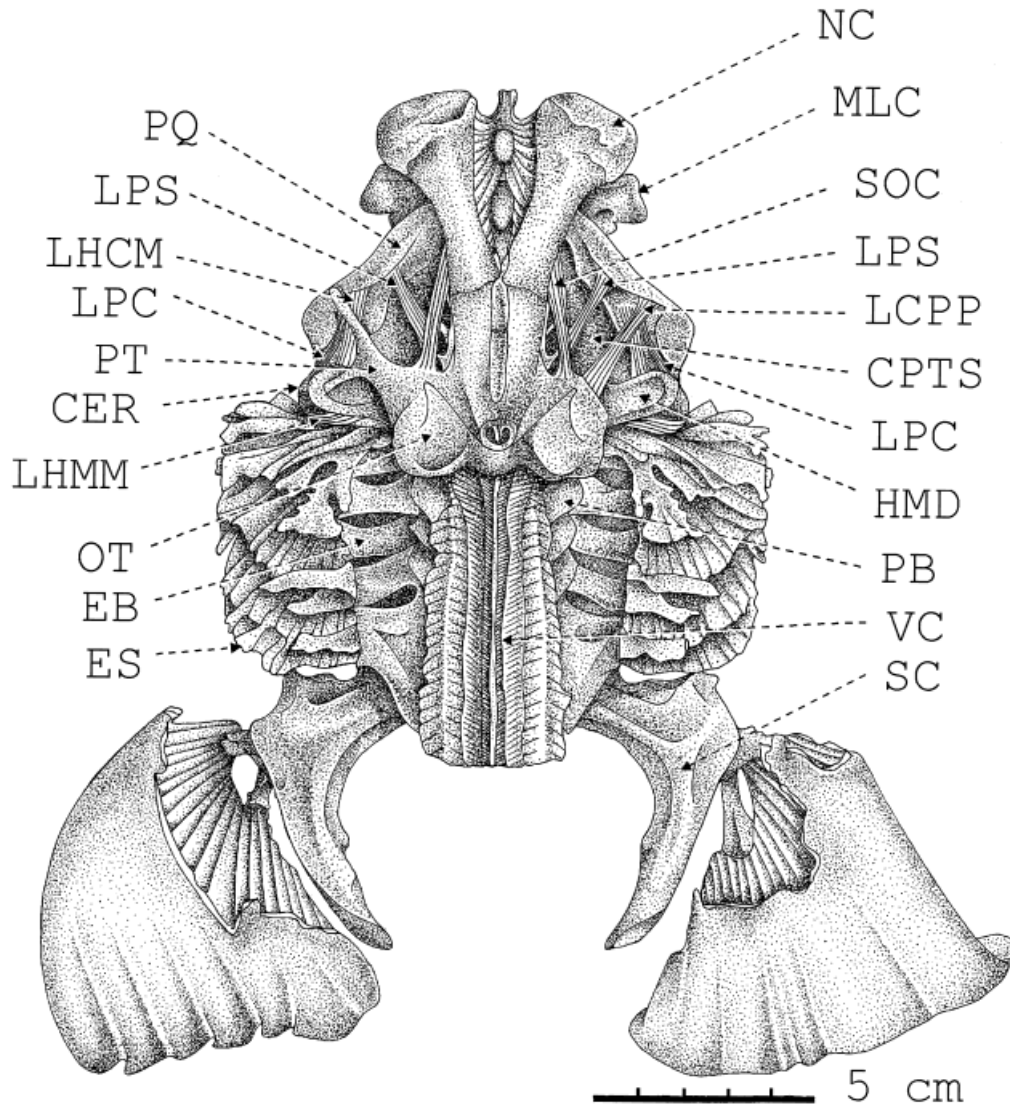


Fig. 8. Dorsal view of the chondrocranium, mandibular, hyoid, and branchial arches and pectoral girdle with pectoral fin of a 79-cm TL male *Ginglymostoma cirratum* with the skin and muscles removed and the right postorbital process removed. Ligaments are indicated. CER, ceratohyal; CPTS, chondrocraniopalatoquadrate connective tissue sheath; EB, extrabranchial cartilage; ES, extra-septalia; HMD, hyomandibula; LCPP, chondrocraniopalatoquadrate ligament (covered by postorbital

process on left side); LHCM, hyomandibuloceratohyomandibular ligament; LHMM, medial hyoidiomandibular ligament; LPC, palatoquadrateceratohyal ligament; LPS, palatoquadrate sheath ligament; MLC, medial labial cartilage; NC, nasal capsule; OT, otic capsule; PB, pharyngobranchial; PQ, palatoquadrate; PT, postorbital process; SC, scapular cartilage; SOC, supraorbital crest; VC, vertebral column.

the superficial head of the posterior division of the preorbitalis. It originates on the antorbital wall, the antorbital shelf, and the rostromedial edge of the postorbital process. The fibers course rostrolaterally to pass over the ascending process of the palatoquadrate,

where it splits into two long tendons. The lateral tendon passes ventrally to merge with the insertional tendon of the anterior division of the preorbitalis. The cranial tendon passes over the dorsal margin of the palatoquadrate, coursing rostrally along its outer

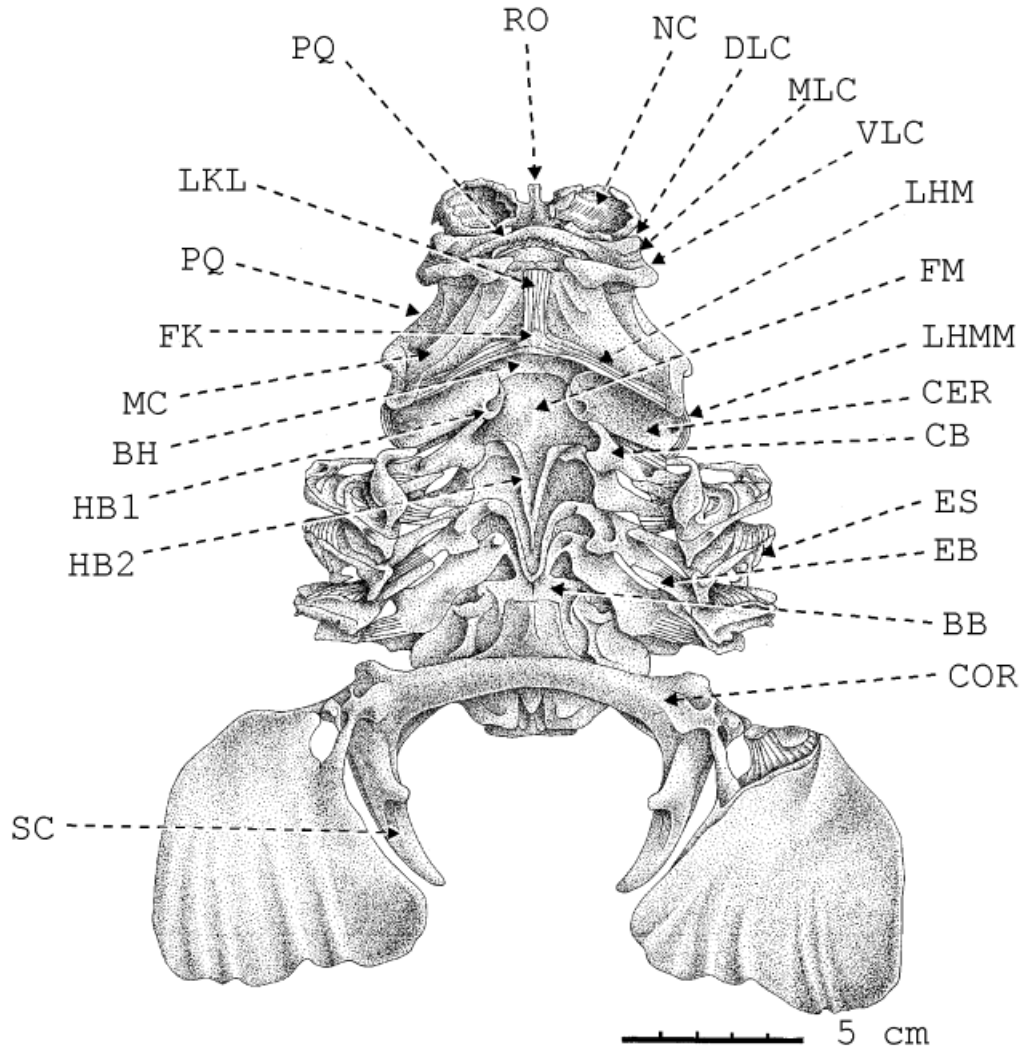


Fig. 9. Ventral view of the chondrocranium, hyoid arch, branchial cartilages, and pectoral girdle of a 79-cm TL male *Ginglymostoma cirratum* with the MHTS removed. BB, basibranchial; BH, basihyal; CB, ceratobranchial; CER, ceratohyal; COR, coracoid; DLC, dorsal labial cartilage; EB, extrabranchial cartilage; ES, extraseptalia; FK, fibrous knob; FM, floor of mouth; HB1, first

hypobranchial; HB2, second hypobranchial; LHM, hyoidiomandibular ligament; LHMM, medial hyoidiomandibular ligament; LKL, knob-labium ligament; MC, mandibular cartilage; MLC, medial labial cartilage; NC, nasal capsule; PQ, palatoquadrate; RO, rostral cartilage; SC, scapular cartilage; VLC, ventral labial cartilage.

surface with some fibers merging with the LPL. The remaining fibers insert on the juncture of the dorsal and medial labial cartilages.

Quadratmandibularis (QM; Figs. 11–13).

This is a complex of five divisions. A broad tendon sheath covers the rostromedial surface of division 4 (QM4), and encases division 2 (QM2), except for its caudal and me-

Fig. 10. Deep dorsal view of the left chondrocranium, mandibular and hyoid arch of a 123-cm TL male *Ginglymostoma cirratum*. The orbit and postorbital process is removed to expose the levator palatoquadrati and spiracularis muscles. APQ, ascending process of palatoquadrate; CER, ceratohyal; DLC, dorsal labial cartilage; EP, epaxialis; HMD, hyomandibula; LCPP, chondrocraniopalatoquadrate ligament; LP, levator palatoquadrati; MLC, medial labial cartilage; NC, nasal capsule; OT, otic capsule; SOC, supraorbital crest; SP, spiracularis.

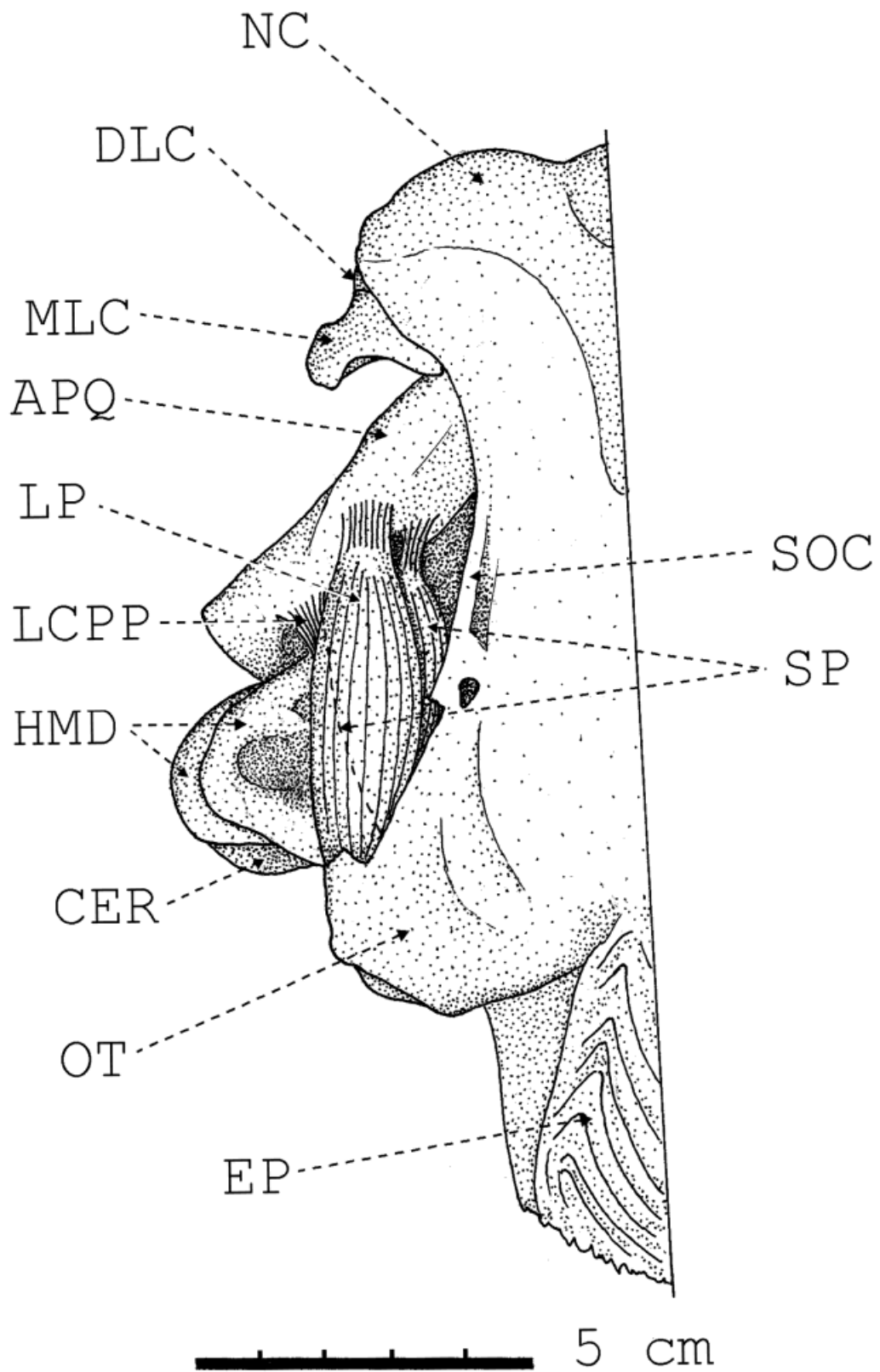


Figure 10

TABLE 2. Synonymies of muscles described for *Ginglymostoma cirratum* and *Negaprion brevirostris* (Motta and Wilga, '95)

Muscle	Vetter (1874, 1878)	Luther ('09)	Allis ('17, '23)	Daniel ('34)	Edgeworth ('35)	Lightoller ('39)	Marinelli & Strenger ('59)	Moss ('72, '77)	Nobiling ('77)	Compagno ('88)
Levator palatoquadrati	L. maxillae superioris	X	L. maxillae superioris	L. maxillae superioris	X	1st levator	X	X, L. maxillae	X	X
Spiracularis	C.S. dorsalis	X, L. palpebrae nictitans		nictitator	spiracularis, L. palpebrae nictitans	pars cranio-maxillaris	X	1st dorsal C.	X	L. palpebrae nictitans
Preorbitalis	L. labii superioris	X	L. labii superioris	L. labii superioris	suborbitalis	X	X	X, intrinsic labial	X	X, L. labii superioris
Quadrato-mandibularis	adductor mandibulae	adductor mandibulae	adductor mandibulae	adductor mandibulae	adductor mandibulae	X	adductor mandibulae	X	adductor mandibulae	X, adductor mandibulae
Intermandibularis	C.S. ventralis	X	X	1st ventral C.	X	X, arcuata mandibularis	X, C. profundus ventralis VII	X	X, C. ventralis	
Levator hyomandibularis	2nd C.S. dorsalis	X	X, L. hyoideus	X, 2nd dorsal C.	X, 2nd dorsal C.	L. hyomandibulae = 2nd levator + pars epihyoidea		X, L. hyoideus	X	X
Constrictor hyoideus dorsalis	2nd C.S. dorsalis	C. dorsalis	2nd C.S. dorsalis	2nd dorsal C.	X	inscriptionalis dorsal	C.S. dorsalis	dorsal C.	C. dorsalis	
Constrictor hyoideus ventralis	2nd C.S. ventralis	C. ventralis	2nd C.S. ventralis	2nd ventral C.	X	inscriptionalis ventralis	C.S. ventralis	ventral C.	C. hyomandibularis	
Interhyoideus	C.S. ventralis		X	2nd ventral C.	C. hyoideus ventralis	interhyoidea	C. profundus ventralis V	X	C. hyomandibularis	
Cucullaris	trapezius	trapezius	trapezius	X, trapezius	cucullaris	L. scapulae	trapezius			X
Coracobranchiales	X		X	X	X		X	X		
Coracoarcualis	coracoarcualis communis		coracoarcualis communis	X, arcus communes	rectus cervicus		coracoarcualis communis			
Coracomandibularis	X	X	X	X, geniocoracoideus	geniocoracoideus		X	X	X	
Coracohyoideus	X		X	X, rectus cervicis	rectus cervicis		X	X		
Epaxialis		dorsal spinale		dorsal bundle	dorsal spinal	dorsal longitudinal bundle	parietalis parepaxonica	X		X

Abbreviations: C., constrictor; L., levator; S., superficialis. X denotes the same nomenclature used in this work and that of Motta and Wilga ('95).

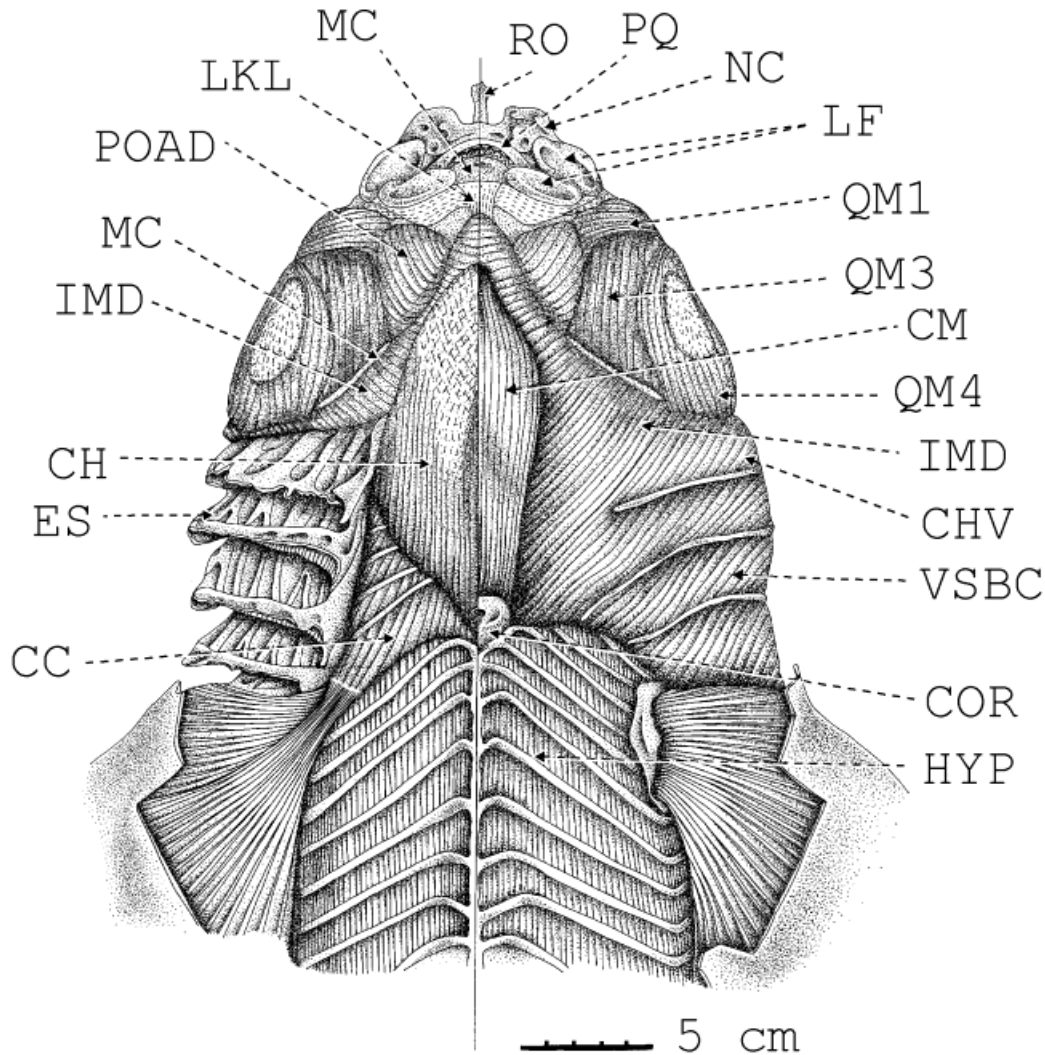


Fig. 11. Ventral view of the head of a 97-cm TL male *Ginglymostoma cirratum* with the skin removed and muscle fiber direction indicated. The intermandibularis and ventral superficial branchial constrictor is cut on both sides to expose deeper muscles. The coracomandibularis is removed on the right side, exposing the deeper corachyoideus. Branchial constrictors are removed on the right side to expose the cartilaginous extra-septalia. CC, coracoarcualis; CH, corachyoideus; CHV, constrictor

tor hyoideus ventralis; CM, coracomandibularis; COR, coracoid; ES, extra-septalia; HYP, hypaxialis; IMD, intermandibularis; LF, labial folds; LKL, knob-labium ligament; MC, mandibular cartilage; NC, nasal capsule; POAD, anterior division of preorbitalis; PQ, palatoquadrate; QM1, quadratomandibularis division 1; QM3, quadratomandibularis division 3; QM4, quadratomandibularis division 4; RO, rostral cartilage; VSBC, ventral superficial branchial constrictor.

dial surfaces. A rostral deep extension of the sheath turns caudomedially to separate QM2 and QM5. The tendon sheath continues rostromedially, deep to divisions 1 and 3, to insert on the lateral surface of the palatoquadrate on and ventral to the ascending process. A slip of this sheath extends ventrally to separate QM1 and QM3. The broad

sheath has several tendinous connections to the overlying skin.

The most rostral division (QM1) originates on the dorsal surface of the palatoquadrate caudal to the ascending process. The fibers run ventrally, wrapping around QM2, to insert by muscular and tendinous connections on the ventral ridge of the mandible,

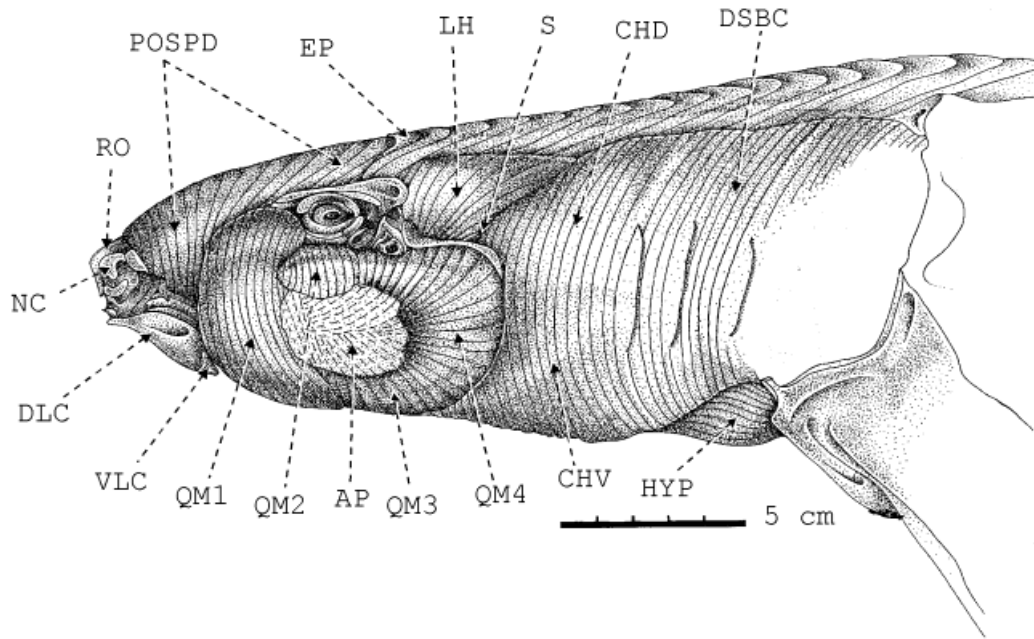


Fig. 12. Left lateral view of the head of a 97-cm TL male *Ginglymostoma cirratum* with the skin removed and the muscle fiber direction indicated. Myosepta of the epaxialis are indicated without fiber direction. AP, aponeurosis over QM2 and QM4; CHD, constrictor hyoideus dorsalis; CHV, constrictor hyoideus ventralis; DLC, dorsal labial cartilage; DSBC, dorsal superficial branchial constrictor; EP, epaxialis; HYP, hypaxialis; LH,

levator hyomandibularis; NC, nasal capsule; POSPD, superficial head of posterior division of preorbitalis; QM1, quadratomandibularis division 1; QM2, quadratomandibularis division 2; QM3, quadratomandibularis division 3; QM4, quadratomandibularis division 4; RO, rostral cartilage; S, spiracle; VLC, ventral labial cartilage.

caudal to the insertion of the superficial head of the posterior division of the preorbitalis. The ventromedial portion is attached to the tendon sheath separating QM1 and QM3.

The second division (QM2), a bipinnate muscle with its apex pointing ventrally, lies between QM1 and QM4. It originates on the broad tendon sheath and the caudolateral surface of the palatoquadrate. It inserts by a broad tendon and a muscular insertion on the lateral rim of the sustentaculum.

The third division (QM3) is a triangular muscle lying between QM1 and QM4, with its apex oriented dorsally. It originates by a muscular and tendinous connection on the caudal portion of the mandibular lateral ridge. Its fibers extend dorsally to insert on the broad tendon sheath that in turn inserts on the lateral surface of the palatoquadrate. The rostral portion is attached to the tendon sheath separating QM1 and QM3.

QM4 is the most caudal division of the quadratomandibularis and overlies the sus-

tentaculum, hyomandibula, and ceratohyal. Its dorsal origin is by a long tendon that is fused to the medial hyoidiomandibular ligament (LHMM) (which in turn is attached to the chondrocranium). A small portion originates from the caudolateral surface of the ceratohyal. Its ventral portion inserts by many small tendons to the caudolateral surface of the sustentaculum. The fibers run rostrally to insert on the broad tendon sheath that inserts on the lateral surface of the palatoquadrate.

The triangular-shaped deep division (QM5, not illustrated) lies within the mandibular fossa. It originates on the ventrolateral surface of the palatoquadrate, ventral to the ascending process, and on the deep extension of the broad tendon sheath. The fibers run ventrally, fanning out to insert on the dorsal surface on the mandibular ridge, the lateral surface of the mandible, and the rostral surface of the sustentaculum.

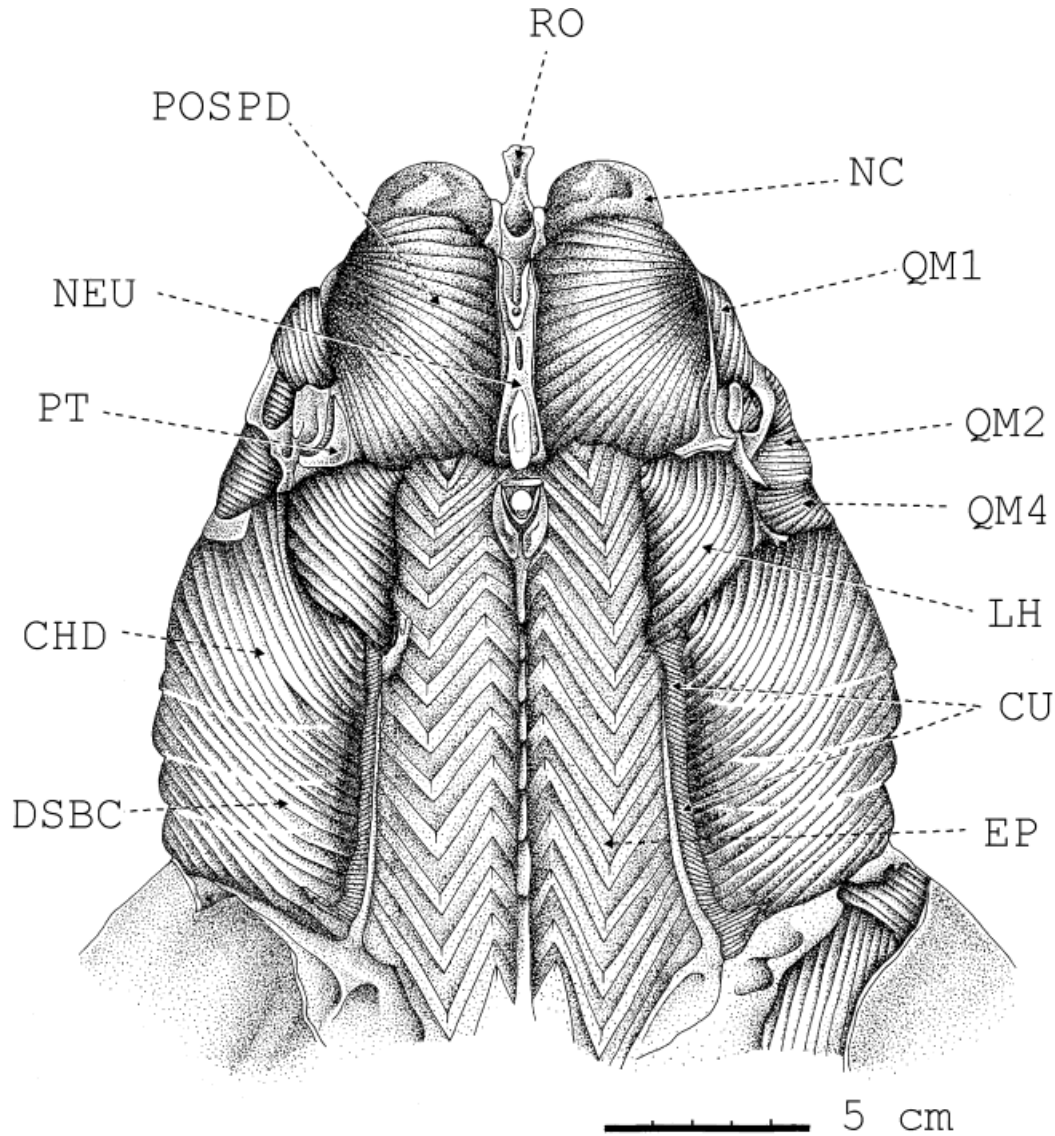


Fig. 13. Dorsal view of the head of a 97-cm TL male *Ginglymostoma cirratum* with the skin removed and muscle fiber direction indicated. Myosepta of the epaxialis are indicated without fiber direction. CHD, constrictor hyoideus dorsalis; CU, cucullaris; DSBC, dorsal superficial branchial constrictor; EP, epaxialis; LH, levator

hyomandibularis; NC, nasal capsule; NEU, neurocranium; POSPD, superficial head of posterior division of preorbitalis; PT, postorbital process; QM1, quadratmandibularis division 1; QM2, quadratmandibularis division 2; QM4, quadratmandibularis division 4; RO, rostral cartilage.

Intermandibularis (IMD; Figs. 11, 14). This originates on the entire ventral rim of the mandible and fascia of the adjacent adductor mandibulae. The rostral-most fibers extend directly to the opposite mandible with no intervening aponeurosis. The remaining

fibers extend caudomedially, inserting on a central aponeurosis that overlies the coracomandibularis and extends as far caudally as the rostral process of the coracoid bar. The caudal two-thirds of the intermandibularis overlies the interhyoideus.

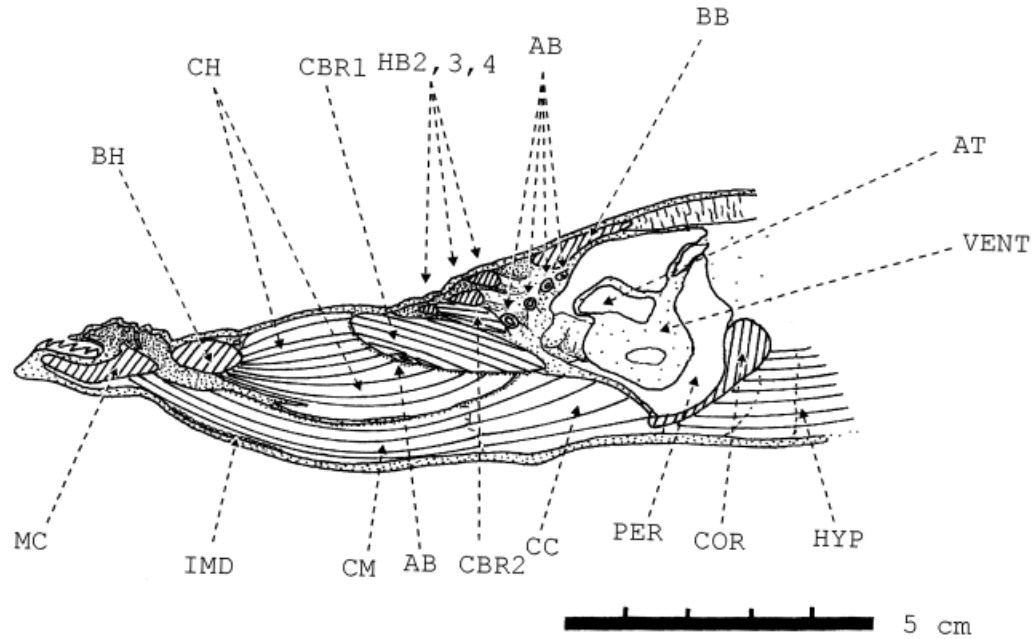


Fig. 14. Sagittal view of the hypobranchial muscles of a 75-cm TL female *Ginglymostoma cirratum*. The view, which is slightly off mid-sagittal, exposes the 1st and 2nd coracobranchiales; the 3rd, 4th, and 5th fan out laterally and are not visible. The thin intermandibularis is deep to the integument only at the rostral end of the coracomandibularis; the interhyoideus is joined by an aponeurosis in the mid-sagittal region and is therefore

not visible. AB, afferent branchial arteries; AT, atrium; BB, basibranchial; BH, hasihyal; CBR1, first coracobranchialis; CBR2, second coracobranchialis; CC, coracoarcualis; CH, coracohyoideus; CM, coracomandibularis; COR, coracoid; HB2,3,4, second, third, fourth hypobranchial; HYP, hypaxialis; IMD, intermandibularis; MC, mandibular cartilage; PER, pericardium; VENT, ventricle.

Muscles of the hyoid muscle plate

Levator hyomandibularis (LH; Figs. 12, 13). Originating on the sphenopteric ridge and on the lateral edge of the epaxialis from the caudal portion of the orbital process to the constrictor hyoideus dorsalis, this muscle inserts on the dorsal and caudodorsal surfaces of the hyomandibula. This muscle is not arranged into superficial and deep heads as in *Negaprion brevirostris* (Motta and Wilga, '95).

Constrictor hyoideus dorsalis (CHD; Figs. 12, 13). This muscle originates on the dorsolateral epaxialis fascia, underlying the LH rostrally. The caudal margin is formed by the first dorsal superficial branchial constrictor and the first branchial cleft. Ventrally, its fibers merge with those of the constrictor hyoideus ventralis. The small spiracle passes through its most rostral margin in the angle formed by QM4 and LH.

Constrictor hyoideus ventralis (CHV; Figs. 11, 12). Its fibers originate on the fascia overlying the coracoarcualis and the myosep-

tum of the ventral portion of the first branchial arch. Rostrally it abuts the caudal margin of the intermandibularis and the interhyoideus. Its fibers continue dorsally to merge with those of the constrictor hyoideus dorsalis.

Interhyoideus (not illustrated). This muscle is thicker than the intermandibularis and lies deep to the caudal two-thirds of the intermandibularis. The interhyoideus originates on the ventral surface of the proximal portion of the ceratohyal. The fibers extend from slightly rostromedial at its rostral end to caudomedial at its caudal end, fanning out to insert on the aponeurosis overlying the coracomandibularis.

Muscles of the branchial muscle plate

Cucullaris (CU; Fig. 13). This originates on the fascia of the lateral surface of the epaxialis and from the scapular process to the otic capsule of the chondrocranium. This muscle is small and thin rostral to the fourth branchial arch, then thickens and

fans out to insert on the cranial surface of the scapular process. A small slip separates from the bulk of the muscle to insert on the dorsal surface of the fifth epibranchial cartilage.

Coracobranchiales (CBR; Fig. 14). There are five of these muscles. The first coracobranchialis is the largest and is fusiform in shape. It originates from the fascia of the rostradorsal surface of the coracoarcualis and extends rostrally to insert by a tendon on the medial end of the first hypobranchial (Figs. 5, 9). The modified first hypobranchial attaches by ligaments to the caudal end of the basihyal near the basihyoceratohyal joint, the caudomedial surface of the ceratohyal, and the rostromedial end of the first ceratobranchial.

The second, third, and fourth coracobranchiales are thin sheet-like muscles, with the two contralateral sides separated by the ventral aorta rostrally and the pericardium caudally. The second coracobranchialis originates on the ventral surface of the rostral portion of the coracoarcualis. The fibers run rostromedially to insert on the caudal surface of the second hypobranchial, the medial surface of the second ceratobranchial, and by a lateral tendon to the ventral surface of the third ceratobranchial at the base of the extrabranchial cartilage (Figs. 9, 14). The third coracobranchialis originates on the ventral surface of the rostral coracoarcualis. The fibers course rostromedially to insert on the caudal surface of the third hypobranchial, the caudomedial surface of the third ceratobranchial, and by a lateral tendon to the ventral surface of the fourth ceratobranchial at the base of the extrabranchial cartilage. The fourth coracobranchialis originates on the caudodorsal surface of the coracoarcualis, the lateral fibrous pericardium, and on the cranioventral surface of the coracoid bar dorsal to the origin of the coracoarcualis. Its caudal-most fibers run rostromedially, narrowing to a fibromuscular neck over the fifth ceratobranchial, then course rostrally to insert on the caudal surface of the fourth hypobranchial, the caudomedial surface of the fourth ceratobranchial, and by a tendon to the ventral surface of the fifth ceratobranchial.

The fifth coracobranchialis lies dorsal to the caudal portion of the fourth coracobranchialis. This muscle has a broad origin on the lateral walls of the fibrous pericardium and the coracoid bar dorsal to the origin of

the fourth coracobranchialis. It runs rostromedially to insert on the ventromedial portion of the fifth ceratobranchial.

Muscles of the hypobranchial muscle plate

Coracoarcualis (CC; Figs. 11, 14). This originates on the lateral surface of the coracoid process, the lateral fibrous pericardium, the cranial surface of the coracoid bar, and the myoseptum separating the cranial edge of the hypaxialis from the coracoarcualis. The muscle extends rostrally to insert at an acute angle on the fascia of the caudal half of the dorsal surface of the coracohyoideus. This muscle is comprised of nine myomeres, with caudodorsally to rostroventrally oriented myosepta throughout its length, and one horizontally oriented dorsal myomere.

Coracomandibularis (CM; Figs. 11, 14).

This unpaired muscle lies deep to the interhyoideus and intermandibularis and superficial to the coracohyoideus and coracoarcualis. The coracomandibularis originates on the cranial surface of the coracoid process and the cranioventral surface of the fibrous pericardium. This caudal portion of the coracomandibularis lies in a V-shaped groove formed by the rostral coracoarcualis and the caudal coracohyoideus. The fibers then extend rostrally and split to form a tendinous insertion on the mandible lateral to the mandibular symphysis and dorsal to the rostral edge of the intermandibularis.

Coracohyoideus (CH; Figs. 11, 14). This paired muscle originates on the ventral surface of the rostral half of the coracoarcualis at an acute angle. Extending rostrally, the right and left muscles fuse at its mid-length. The muscle inserts on the ventromedial surface of the ceratohyobasihyal joint and the caudal and ventral surfaces of the basihyal by means of a broad muscular insertion and a thick ventral tendon sheath. Some of the tendons of insertion cross to the contralateral side.

Axial muscle

Epaxialis (EP; Figs. 12, 13). This group inserts on the dorsal surface of the otic capsule. The cranial margin is the rostral edge of the postorbital process and the caudal portion of the supraorbital crest, the lateral margin is the sphenopterotic ridge, and its medial margin is the parietal fossa.

DISCUSSION

Suspensorium and jaw kinesis

The palatoquadrate cartilages of *Ginglymostoma cirratum* articulate indirectly with the chondrocranium caudally through the hyomandibulae, and directly by means of the ethmoorbital articulations rostrally (Maisey, '80; Compagno, '88; Motta and Wilga, '95). The ethmoorbital articulation consists in part of the ethmopalatine joint, in which the small, orbital process of the palatoquadrate is bound to the ethmoid region of the chondrocranium by a short, thin ethmopalatine ligament. The orbital process articulates with a groove formed by the lateral edge of the antorbital shelf. The type of orbital process and the bracing of the palatoquadrate against the cranium in *G. cirratum* appears to be a derived character shared with the heterodontoids (Compagno, '77, '88). Furthermore, in the closed, retracted position the palatine process of the palatoquadrate rests against the ventral surfaces of the nasal capsule and the ascending process of the palatoquadrate rests against the rostro-dorsal end of the suborbital shelf (see also Compagno, '73). When the jaw is maximally open and the palatoquadrate protrudes, the orbital process of the palatoquadrate glides in the groove formed by the lateral edge of the antorbital shelf such that the palatoquadrate moves away from its support on the neurocranium rostrally. Together, the ethmopalatine ligament and the chondrocraniopalatoquadrate connective tissue sheath permit only slight rostroventral protrusion of the palatoquadrate.

The caudal jaw articulation of *Ginglymostoma cirratum* is stabilized by short and stout hyomandibulae (Moss, '77), a complex series of ligaments, and indirectly by the skin and muscles. The hyomandibulochondrocranial joint is composed of rostral and caudal condyles that sit in approximately ellipsoidal sockets. This prevents twisting of the hyomandibulae about their longitudinal axes, yet allows the hyomandibulae to pivot rostroventrally. Distally, the hyomandibulae have a diarthrodial articulation with a shallow socket on the mandibular knob and a fibrous joint with the proximal ceratohyal. The hyomandibulomandibuloceratohyal union is tightly bound by numerous ligaments, including the thick medial hyoidiomandibular ligament (LHMM) that courses from the chondrocranium and hyoman-

dibula, wrapping around the proximal ceratohyal to insert on the mandible.

As the mandible depresses and the palatoquadrate protrudes slightly, the distal end of the hyomandibula pivots ventrally and slightly rostrally, the distal end of the ceratohyal pivots caudoventrally, and the basihyal moves from its rostral position just caudal to the mandibular symphysis to a more caudoventral position. Consequently, the floor of the mouth is depressed, increasing the buccal volume. We did not detect any noticeable change in the angle formed by the mandibles during maximum jaw opening (during manual manipulation) as reported for *Orectolobus maculatus* by Wu ('94). He proposed a method of jaw protrusion in orectolobiform sharks involving lateral compression of the jaw joints by means of the interhyoideus. This is hypothesized to squeeze the palatoquadrate cartilages together, as well as the mandibular cartilages, effectively increasing their length as their angles become more acute. Moss ('65, '77) previously proposed a mechanism of palatoquadrate protrusion in *Ginglymostoma cirratum* involving contraction of the quadratomandibularis muscle as well as the anterior division of the preorbitalis, such that the palatoquadrate is pulled ventrally towards the abducted mandible. Electromyographic and kinematic experiments should, therefore, reveal contraction of the interhyoideus coincident with palatoquadrate protrusion, along with a significant decrease in the angle subtended by the mandibular cartilages according to Wu's ('94) model, whereas, according to Moss ('77), protrusion would be coincident with contraction of the preorbitalis anterior and the quadratomandibularis (but see Preorbitalis, below). In the latter case, the interhyoideus would most likely be active after the initiation of palatoquadrate protrusion, perhaps during the compressive phase when the mandible is being adducted, as occurs during the compressive phase of respiration in the dogfish, *Scyliorhinus canicula* (Hughes and Ballintijn, '65). In addition, there should be minimal change in the angle subtended by the mandibular cartilages. Verification of this awaits our electromyographic and kinematic analyses.

Ginglymostoma cirratum has a double articulation of the quadratomandibular joint, characteristic of cladodont level sharks (Schaeffer, '67). Cladodont level sharks had extensive bracing of the palatoquadrate on

the neurocranium, yet also had a double quadratomandibular joint, although it is not clear as to the extent of stability conferred by the joint (Schaeffer, '67; Moy-Thomas and Miles, '71). In *G. cirratum*, the lateral quadratomandibular joint lies in a frontal plane. This joint is ellipsoidal, such that it resists lateral movement between the mandible and the palatoquadrate. The medial quadratomandibular joint lies rostromedial to the latter joint and lies in the sagittal plane, further restricting lateral displacement of the jaws. The medial quadratomandibular joint is similar to a gliding joint in having a shallow fossa in the palatoquadrate and a small, circular condyle on the mandible. Similar to *Negaprion brevirostris* (Motta and Wilga, '95), this joint, along with numerous ligaments such as the inner quadratomandibular ligament (LQI), stabilize the mandible on the palatoquadrate.

Musculature

The musculature of numerous sharks has been described (reviewed by Motta and Wilga, '95), with descriptions of orectolobiform muscles by Denison ('37), Lightoller ('39), Moss ('65, '77), Gilbert ('70), and Wu ('94). Two muscle groups require further discussion.

Preorbitalis

Ginglymostoma cirratum has a single preorbitalis similar to other orectolobiform sharks (Lightoller, '39; Compagno, '73, '88). The muscle is divided into anterior and posterior divisions (Moss, '65). The broad origin of the posterior division on the dorsal surface of the neurocranium, and the origin of the anterior division on the mandible rostral to the quadratomandibularis, is considered a derived condition (Compagno, '88; deCarvalho, '96; Shirai, '92, '96). Moss ('65, '77) described an insertion of the anterior division of the preorbitalis onto the palatoquadrate in *G. cirratum*, a finding we could not substantiate. We believe this insertion is unlikely, as this is a derived condition found only in carcharhiniform sharks. In carcharhiniform sharks the preorbitalis is divided into a preorbitalis dorsal and ventral. The dorsal preorbitalis originates from the quadratomandibularis in common with the ventral division, but extends horizontally and rostrally to insert on the palatoquadrate rather than the nasal region (Moss, '72; Compagno, '88; Motta and Wilga, '95). Contraction

of the dorsal and ventral preorbitalis in carcharhinid sharks is involved with protrusion of the palatoquadrate (Motta et al., '97).

In *Ginglymostoma cirratum*, the anterior division of the preorbitalis inserts on the ventral labial cartilage, labial fold, and merges with the insertional tendon of the deep head of the posterior division of the preorbitalis. The deep head of the posterior division of the preorbitalis also partially inserts on the dorsal and medial labial cartilages. Therefore, it appears that contraction of the preorbitalis in *G. cirratum* may not assist palatoquadrate protrusion as suggested by Moss ('77) and Wu ('94); rather, it may contribute to closure of the jaws during crushing of its hard prey, as it does in the batoid guitarfish *Rhinobatos lentiginosus* (Bell and Nichols, '21; Gudger, '21; Bigelow and Schroeder, '48; Castro, '83; Compagno, '84; Wilga and Motta, '98b), and perhaps retraction of the labial cartilages as the mouth is closing. A vertically oriented preorbitalis is shared by orectolobiform and heterodontiform sharks, in contrast to carcharhiniform, lamniform, and squaliform sharks, in which it is horizontally oriented (Luther, '09; Edgeworth, '35; Compagno, '88; Shirai, '96).

Levator palatoquadrati and spiracularis

The levator palatoquadrati and spiracularis (first dorsal constrictor) are distinct muscles that lie deep to the orbital region in *Ginglymostoma cirratum*. This agrees with Lightoller ('39), Compagno ('88), and Shirai ('96), who found the spiracularis to be separate from the levator palatoquadrati in *Orectolobus*, but differs with deCarvalho ('96), who states that orectolobiforms have a spiracularis not separated from the levator palatoquadrati.

The small and localized origin of the levator palatoquadrati in the region of the postorbital process in *Ginglymostoma cirratum* is believed to reflect the ancestral condition (Nakaya, '75). Unlike the vertically oriented ancestral condition in which it inserts onto the mid-dorsal surface of the palatoquadrate, such as in the spiny dogfish *Squalus acanthias* (Nakaya, '75; Wilga and Motta, '98a), the levator palatoquadrati in *G. cirratum* extends rostrally to insert onto the rostradorsal surface of the palatoquadrate, resulting in the horizontal orientation of the muscle. In contrast, the levator palatoquadrati of *Negaprion brevirostris*, as in most carcharhinids, originates from the orbit of

the preorbital wall, across the supraorbital region to the postorbital process, and extends caudally to insert on the mid-dorsal region of the palatoquadrate (Motta and Wilga, '95). As such, the obliquely oriented levator palatoquadrati, along with the preorbitalis, assists palatoquadrate protrusion by pulling the palatoquadrate rostrorodorsally (Motta et al., '97). Due to the caudal origin and rostral insertion of the levator palatoquadrati (and spiracularis) in *G. cirratum*, its contraction can only result in retraction of the palatoquadrate, and we suspect it contracts during the recovery phase of jaw kinematics during feeding.

Functional modifications for suction feeding

Specialization for capturing prey by suction has repeatedly arisen in numerous elasmobranch taxa. Within the orectolobiforms, suction feeding is the dominant form of prey capture (Tanaka, '73; Russo, '75; Talent, '76; Moss, '77; Tricas, '82; Castro, '83; Compagno, '84, '90; Strong, '89; Fouts, '94; Wu, '94; Clark and Nelson, '97; Wilga and Motta, '98a). The nurse shark, *Ginglymostoma cirratum* is a benthic feeder that locates its prey primarily by olfactory and gustatory gradient searching or klinotaxis (Gilbert, '70; Hodgson and Mathewson, '71). Its prey of benthic invertebrates and small fish (Bell and Nichols, '21; Gudger, '21; Bigelow and Schroeder, '48; Castro, '83; Compagno, '84) is either transported directly into the pharynx during the suction capture, or crushed by the teeth after the initial suction capture. The suction capture may be so powerful as to dismember portions of the prey (personal observation).

Morphological specializations for suction feeding in this species include apparently hypertrophied depressor muscles of the hyoid and branchial arches when compared to carcharhinid sharks (Moss, '65, '77), notably the coracohyoideus and coracobranchiales, small mouth with well-developed labial cartilages that laterally enclose the mouth, teeth reduced in size, and generation of large subambient suction pressures (Bigelow and Schroeder, '48; Compagno, '73; Tanaka, '73; Moss, '77; Dingerkus, '86; Wu, '94). In addition, the mouth is close to the tip of the snout (Bigelow and Schroeder, '48) and functionally terminal when maximally open, a derived character of orectoloboids (Compagno, '88). Although we did not quantify hypertrophy of the depressor muscles (Moss, '65, '77), the coracohyoideus and first coracobranchialis appear hypertrophied as compared to

Negaprion brevirostris, a ram-feeding carcharhinid shark (Motta and Wilga, '95; Motta et al., '97).

Advanced teleosts specialized for suction prey capture show convergence in many of these characters, including small or no teeth that do not interfere with water inflow into the mouth, rapid buccal expansion, and a protrusible upper jaw that creates a small, terminal, and laterally enclosed mouth (Alexander, '74; Lauder, '79, '85; Liem, '80, '93; Motta, '84, '85, '88; Muller and Osse, '84). Formation of a circular, laterally enclosed orifice during suction capture is important for directing the streamlines cranially (Alexander, '74; Lauder, '79, '85; Muller et al., '82; Muller and Osse, '84).

During prey capture, the mouth of *Ginglymostoma cirratum* forms a somewhat round, laterally enclosed aperture. This is primarily due to the three prominent labial cartilages that border the rostralateral margins of the mouth, and less to palatoquadrate protrusion. During maximum jaw opening the ligamentous connections of the dorsal and ventral labial cartilages to the palatoquadrate and mandible respectively, and their connections to the medial labial cartilage result in the labial cartilages swinging into an almost vertical orientation. Together with the PMTS, they laterally occlude the mouth. Occlusion of the lateral sides of the gape by the labial cartilages also occurs in the suction feeding dogfish, *Squalus acanthias*, and leopard shark, *Triakis semifasciata* (Ferry-Graham, '98a; Wilga and Motta, '98a). In *G. cirratum*, a medially directed process of the medial labial cartilage abuts the palatoquadrate, holding the labial cartilages away from the jaws. This mechanical stay may be important in bracing the labial cartilages during the powerful subambient suction forces, preventing their collapse into the oral aperture.

Moss ('65, '77) reported a prominent intrinsic muscle of the labial cartilages, passing from the caudal face of the ventral cartilage to the caudal face of the medial cartilage. This muscle supposedly extends the labial cartilages, producing the almost tubular mouth opening. Repeated dissection, even of large adult (252 cm TL) *Ginglymostoma cirratum*, failed to discern this muscle. We believe Moss' intrinsic labial muscle is part of the anterior division of the preorbitalis (see Preorbitalis). Rostral pivoting of the labial cartilages in *G. cirratum* may be mechanically linked to depression of the mandible by their ligamentous connections.

ACKNOWLEDGMENTS

We are grateful for donation of time and materials from many persons and institutions. Generous assistance in anatomical preparation by Rebecca Carr, Amelia Griffith, Emily Minor and Toni Pietrzak is appreciated. Ellen Padgett and University Diagnostics donated time and material for the CAT scans. Hannah Spear prepared most of the original artwork. Eric Sander, James Bonnel, Carl Luer, Keys Marine Laboratory, and Mote Marine Laboratory donated specimens. Mote Marine Laboratory and the University of South Florida provided facilities and expertise. We thank Richard Lund and Eileen Grogan and two anonymous reviewers for providing critical comments on the manuscript. This project was supported by a grant from the National Science Foundation to P.J.M. (DEB 9117371).

LITERATURE CITED

- Alexander R McN. 1974. Functional design in fishes. London: Hutchinson University Library.
- Allis EP Jr. 1913. The homologies of the ethmoidal region of the Selachian skull. *Anat Anz* 44:322–328.
- Allis EP Jr. 1914. Certain homologies of the palatoquadrate of Selachian. *Anat Anz* 45:353–373.
- Allis EP Jr. 1915. The homologies of the hyomandibula of the gnathostome fishes. *J Morphol* 26:562–624.
- Allis EP Jr. 1917. The homologies of the muscles related to the visceral arches of the gnathostome fishes. *Q J Microsc Sci* 62:303–406.
- Allis EP Jr. 1923. The cranial anatomy of *Chlamydoselachus anguineus*. *Acta Zool* 4:123–221.
- Bell JC, and JT Nichols. 1921. Notes on the food of Carolina sharks. *Copeia* 1921:17–20.
- Bigelow HB, Schroeder WC. 1948. Fishes of the western North Atlantic. Part 1. New Haven: Sears Foundation for Marine Research.
- Carroll RL. 1988. Vertebrate paleontology and evolution. New York: WH Freeman.
- Castro JI. 1983. The sharks of North American waters. College Station: Texas A&M University Press.
- Clark E, Nelson DR. 1997. Young whale sharks, *Rhincodon typus*, feeding on a copepod bloom near La Paz, Mexico. *Environ Biol Fish* 50:63–73.
- Compagno LJV. 1973. Interrelationships of living elasmobranchs. In: Greenwood PH, Miles RS, Patterson C, editors. Interrelationships of fishes. *Zool J Linn Soc Suppl* 1 53:15–61.
- Compagno LJV. 1977. Phyletic relationships of living sharks and rays. *Am Zool* 17:303–322.
- Compagno LJV. 1984. FAO species catalogue. Vol 4. Sharks of the world. An annotated and illustrated catalogue of sharks species known to date. Part 1. Hexanchiformes to Lamniformes. FAO Fish Synop 125. 249 p.
- Compagno LJV. 1988. Sharks of the order Carcharhiniformes. Princeton: Princeton University Press.
- Compagno LJV. 1990. Relationships of the megamouth shark, *Megachasma pelagios* (Lamniformes: Megachasmidae), with comments on its feeding habits. In: Pratt HL Jr, Gruber SH, Taniuchi T, editors. Elasmobranchs as living resources: advances in the biology, ecology, systematics, and the status of the fisheries: NOAA technical report. National Marine Fisheries Service 90. p 357–379.
- Daniel JF. 1915. The anatomy of *Heterodontus francisci*. II. The endoskeleton. *J Morphol* 26:447–493.
- Daniel JF. 1934. The elasmobranch fishes. Berkeley: University of California Press.
- deCarvalho MR. 1996. Higher level elasmobranch phylogeny, basal squalians, and paraphyly. In: Stiassny MLJ, Parenti LR, Johnson GD, editors. Interrelationships of fishes. New York: Academic Press. p 35–62.
- Denison RH. 1937. Anatomy of the head and pelvic fin of the whale shark, *Rhineodon*. *Am Mus Nat Hist* 73:477–515.
- Dingerkus G. 1986. Interrelationships of orectolobiform sharks (Chondrichthyes: Selachii). In: Uyeno T, Arai R, Taniuchi T, Matsuura K, editors. Indo-Pacific fish biology: proceedings of the Second International Conference on Indo-Pacific Fishes. Tokyo: Ichthyological Society of Japan. p 227–245.
- Edgeworth FH. 1935. Cranial muscles of vertebrates. Cambridge: Cambridge University Press.
- Ferry-Graham LA. 1997. Feeding kinematics of juvenile swellsharks, *Cephaloscyllium ventriosum*. *J Exp Biol* 200:1255–1269.
- Ferry-Graham LA. 1998a. Effects of prey size and mobility on prey-capture kinematics in leopard sharks *Triakis semifasciata*. *J Exp Biol* 201:2433–2444.
- Ferry-Graham LA. 1998b. Feeding kinematics of hatching swellsharks, *Cephaloscyllium ventriosum* (Scyliorhinidae): the importance of predator size. *Mar Biol* 131:703–718.
- Fouts WR. 1994. Predatory behavior of the Pacific angel shark, *Squatina californica*: visually-mediated attacks and ambush site characteristics. *Am Soc Ichthyol Herp June* 2–8, University of Southern California, Los Angeles (Abstract).
- Gadow H. 1888. On the modifications of the first and second visceral arches, with special reference to the homologies of the auditory ossicles. *Philos Trans R Soc Lond* 179B:451–485.
- Gegenbaur C. 1865. Untersuchungen zur vergleichenden Anatomie der Wirbelthiere. Zweites Heft. 1. Schultergürtel der Wirbelthiere. 2. Brustflosse der Fische. Leipzig: Wilhelm Engelmann.
- Gegenbaur C. 1872. Untersuchungen zur vergleichenden Anatomie der Wirbelthiere. Drittes Heft. Das Kopfskelet der Selachier, ein Beitrag zur Erkenntnis der Genese des Kopfskeletes der Wirbelthiere. Leipzig: Wilhelm Engelmann.
- Gilbert PW. 1970. Studies on the anatomy, physiology, and behavior of sharks. Office of Naval Research Final Rep Project No 104–471, p 1–45.
- Goodey T. 1910. A contribution to the skeletal anatomy of the frilled shark, *Chlamydoselachus anguineus* (Gar). *Proc Zool Soc Lond* 2:540–571.
- Gudger EW. 1921. Notes on the morphology and habits of the nurse shark, *Ginglymostoma cirratum*. *Copeia* 1921:57–59.
- Hodgson ES, Mathewson RF. 1971. Chemosensory orientation in sharks. *Ann NY Acad Sci* 188:175–182.
- Hughes GM, Ballintijn CM. 1965. The muscular basis of the respiratory pumps in the dogfish (*Scyliorhinus canicula*). *J Exp Biol* 43:363–383.
- Lauder GV. 1979. Feeding mechanics in primitive teleosts and in the halecomorph fish *Amia calva*. *J Zool Lond* 187:543–578.
- Lauder GV. 1982. Patterns of evolution in the feeding mechanism of actinopterygian fishes. *Am Zool* 22:275–285.
- Lauder GV. 1985. Aquatic feeding in lower vertebrates. In: Hildebrand M, Bramble DM, Liem KF, Wake DB, editors. Functional vertebrate morphology. Cambridge: Harvard University Press.
- Lauder GV, Reilly SM. 1988. Functional design of the feeding mechanism in salamanders: causal bases of

- ontogenetic changes in function. *J Exp Biol* 134:219–233.
- Liem KF. 1980. Acquisition of energy by teleosts: adaptive mechanisms and evolutionary patterns. In: Ali MA, editor. *Environmental physiology of fishes*. New York: Plenum. p 299–334.
- Liem KF. 1993. Ecomorphology of the teleostean skull. In: Hanken J, Hall BK, editors. *The skull functional and evolutionary mechanisms*, vol. 3. Chicago: University of Chicago Press. p 422–452.
- Lightoller GHS. 1939. Probable homologues. A study of the comparative anatomy of the mandibular and hyoid arches and their musculature. I. Comparative morphology. *Trans Zool Soc Lond* 24:349–444.
- Lund R. 1985. Stethacanthid elasmobranch remains from the Bear Gulch limestone (Namurian E2b) of Montana. *Am Mus Nov* 2828:1–24.
- Lund R, Grogan ED. 1997. Relationships of the Chimaeriformes and the basal radiation of the Chondrichthyes. *Rev Fish Biol Fisheries* 7:65–123.
- Luther A. 1909. Untersuchungen über die vom *N. trigeminus* innervierte Muskulatur der Selachier (Haie und Rochen) unter Berücksichtigung ihrer Beziehungen zu benachbarten Organen. *Acta Soc Sci Fenn* 36:1–176.
- Maisey JG. 1980. An evaluation of jaw suspension in sharks. *Am Mus Nov* 2706:1–17.
- Marinelli W, Strenger A. 1959. Vergleichende Anatomie und Morphologie der Wirbeltiere III Lieferung (*Squalus acanthias*). Vienna: Franz Deuticke.
- Miyake T, McEachran JD, Hall BK. 1992. Edgeworth's legacy of cranial muscle development with an analysis of muscles in the ventral gill arch region of batoid fishes (Chondrichthyes: Batoidea). *J Morphol* 212:213–256.
- Moss SA. 1965. The feeding mechanisms of three sharks: *Galeocerdo cuvieri* (Peron & Le Sueur), *Negaprion brevirostris* (Poey), and *Ginglymostoma cirratum* (Bonaterre). Cornell University dissertation.
- Moss SA. 1972. The feeding mechanism of sharks of the family Carcharhinidae. *J Zool Lond* 167:423–436.
- Moss SA. 1977. Feeding mechanisms in sharks. *Am Zool* 17:355–364.
- Motta PJ. 1984. The mechanics and functions of jaw protrusion in teleost fishes: a review. *Copeia* 1984:1–18.
- Motta PJ. 1985. Functional morphology of the head of Hawaiian and Mid-Pacific butterflyfishes (Perciformes, Chaetodontidae). *Environ Biol Fish* 13:253–276.
- Motta PJ. 1988. Functional morphology of the feeding apparatus of ten species of Pacific butterflyfishes (Perciformes, Chaetodontidae): an ecomorphological approach. *Environ Biol Fish* 22:39–67.
- Motta PJ, Wilga CAD. 1995. Anatomy of the feeding apparatus of the lemon shark, *Negaprion brevirostris*. *J Morphol* 226:309–329.
- Motta PJ, Tricas TC, Hueter RE, Summers AP. 1997. Feeding mechanism and functional morphology of the jaws of the lemon shark *Negaprion brevirostris* (Chondrichthyes, Carcharhinidae). *J Exp Biol* 200:2765–2780.
- Moy-Thomas JA, Miles RS. 1971. *Paleozoic fishes*. London: Chapman & Hall.
- Muller M, Osse JWM. 1984. Hydrodynamics of suction feeding in fish. *Trans Zool Soc Lond* 37:51–135.
- Muller M, Osse JWM, Verhagen JHG. 1982. A quantitative hydrodynamic model of suction feeding in fish. *J Theor Biol* 95:49–79.
- Nakaya K. 1975. Taxonomy, comparative anatomy and phylogeny of Japanese catsharks, Scyliorhinidae. *Mem Fac Fish Hokkaido Univ* 23:1–94.
- Nobiling G. 1977. Die Biomechanik des Kieferapparates beim Stierkopfhai (*Heterodontus portusjacksoni* = *Heterodontus philippi*). *Adv Anat Embryol Cell Biol* 52:1–52.
- Parker WK. 1878. On the structure and development of the skull in sharks and skates. *Trans Zool Soc Lond* 10:189–234.
- Reilly SM. 1995. The ontogeny of aquatic feeding behavior in *Salamandra salamandra*: stereotypy and isometry in feeding kinematics. *J Exp Biol* 198:701–708.
- Ridewood WG. 1895. On the spiracle and associated structures in elasmobranch fishes. *Anat Anz* 2:425–433.
- Romer AS. 1966. *Vertebrate paleontology*. Chicago: University of Chicago Press.
- Russo RA. 1975. Observations on the food habits of leopard sharks (*Triakis semifasciata*) and brown smooth-hounds (*Mustelus henle*). *Calif Fish Game* 61:95–103.
- Schaeffer B. 1967. Comments on elasmobranch evolution. In: Gilbert PW, Mathewson RF, Rall DP, editors. *Sharks, skates, and rays*. Baltimore: Johns Hopkins Press. p 3–35.
- Schaeffer B, Williams M. 1977. Relationship of fossil and living elasmobranchs. *Am Zool* 17:293–302.
- Shirai S. 1992. Squalan phylogeny: a new framework of "squaloid" sharks and related taxa. Sapporo: Hokkaido University Press.
- Shirai S. 1996. Phylogenetic interrelationships of neoselachians (Chondrichthyes: Euselachii). In: Stiassny MLJ, Parenti LR, Johnson GD, editors. *Interrelationships of fishes*. New York: Academic Press. p 9–34.
- Strong WR Jr. 1989. Behavioral ecology of horn sharks, *Heterodontus francisci*, at Santa Catalina Island, California, with emphasis on patterns of space utilization. California State University thesis.
- Talent LG. 1976. Food habits of the leopard shark, *Triakis semifasciata*, in Elkhorn Slough, Monterey Bay, California. *Calif Fish Game* 62:286–298.
- Tanaka SK. 1973. Suction feeding by the nurse shark. *Copeia* 1973:606–608.
- Tricas TC. 1982. Bioelectric-mediated predation by swell sharks, *Cephaloscyllium ventriosum*. *Copeia* 1982:948–952.
- Vetter B. 1874. Untersuchungen zur vergleichenden Anatomie der Kiemen- und Kiefermuskulatur der Fische. *Jena Zeitschr f Naturw* 8:405–458.
- Vetter B. 1878. Untersuchungen zur vergleichenden Anatomie der Kiemen- und Kiefermuskulatur der Fische. *Jena Zeitschr f Naturw* 12:431–550.
- Wainwright PC, Sanford CP, Reilly SM, Lauder GV. 1989. Evolution of motor patterns: aquatic feeding in salamanders and ray-finned fishes. *Brain Behav Evol* 34:329–341.
- Wilga CD, Motta PJ. 1998a. Conservation and variation in the feeding mechanism of the spiny dogfish, *Squalus acanthias*. *J Exp Biol* 201:1345–1358.
- Wilga CD, Motta PJ. 1998b. Feeding mechanism of the Atlantic guitarfish *Rhinobatus lentiginosus*: modulation of kinematic and motor activity. *J Exp Biol* 201:3167–3184.
- Wu EH. 1994. A kinematic analysis of jaw protrusion in orectolobiform sharks: a new mechanism for jaw protrusion in elasmobranchs. *J Morphol* 222:175–190.
- Zangerl R. 1981. Chondrichthyes. I. Paleozoic Elasmobranchii. In: Schultze HP, editor. *Handbook of paleoichthyology*, 3A. Stuttgart: Gustav Fischer Verlag.